ISTANBUL TECHNICAL UNIVERSITY ★ GRADUATE SCHOOL OF SCIENCE ENGINEERING AND TECHNOLOGY

ENERGY-BASED METRICS FOR FIGHTER AIRCRAFT ASSESSMENT

M.Sc. THESIS

Nazmia HUMAIRA

Department of Aeronautics and Astronautics Engineering

Aeronautics and Astronautics Engineering Programme

JUNE 2018

ISTANBUL TECHNICAL UNIVERSITY ★ GRADUATE SCHOOL OF SCIENCE ENGINEERING AND TECHNOLOGY

ENERGY-BASED METRICS FOR FIGHTER AIRCRAFT ASSESSMENT

M.Sc. THESIS

Nazmia HUMAIRA
(511151153)

Department of Aeronautics and Astronautics Engineering

Aeronautics and Astronautics Engineering Programme

Thesis Advisor: Assist. Prof. Dr. Emre KOYUNCU

JUNE 2018

İSTANBUL TEKNİK ÜNİVERSİTESİ ★ FEN BİLİMLERİ ENSTİTÜSÜ

SAVAŞ UÇAĞI DEĞERLENDİRMESİ İÇİN ENERJİ TABANLI METRİKLER

YÜKSEK LİSANS TEZİ

Nazmia HUMAIRA
(511151153)

Uçak ve Uzay Mühendisliği Anabilim Dalı

Uçak ve Uzay Mühendisliği Programı

Tez Danışmanı: Assist. Prof. Dr. Emre KOYUNCU

HAZİRAN 2018

Nazmia HUMAIRA, a M.Sc. student of ITU Graduate School of Science Engineering and Technology 511151153 successfully defended the thesis entitled "ENERGY-BASED METRICS FOR FIGHTER AIRCRAFT ASSESSMENT", which he/she prepared after fulfilling the requirements specified in the associated legislations, before the jury whose signatures are below.

Thesis Advisor :	**Assist. Prof. Dr. Emre KOYUNCU** Istanbul Technical University	.....
Jury Members :	**Prof. Dr. Gökhan İNALHAN** Istanbul Technical University	.....
	Assist. Prof. Dr. Emre KOYUNCU Istanbul Technical University	.....
	Dr. Umut DEMIREZEN STM Savunma Teknolojileri	.....

Date of Submission : **3 May 2018**
Date of Defense : **5 June 2018**

For my best teachers: my mother and my father

FOREWORD

I would like to express my biggest gratitude to my thesis advisor, Prof. Emre Koyuncu, for all his guidances during my graduate study. I would like to express my deepest acknowledgement to my unofficial thesis advisor, Captain Firman D.C. M.A., for giving me many perspectives on realistic aerial combat. I would like to thank everyone in the Control and Avionics Research Group of ITU ARC, especially Barış Başpınar and Mevlüt Uzun for their helps since 312A.

All the efforts that I did for this thesis would never be enough without the supports of my first teachers: my mother, Siti Nadroh and my father, Humaedi Hasan. I would like to thank my sisters, Zahra Medina in Paris, France and Samira Dial Megistra in Saint Petersburg, Russia because without their supports and sweet laughters, I would never have enough spirit to finish this thesis.

I would like to thank the dearest husband in the world, Bekir Usinov, for all the lessons, jokes, and laughters that we share together. Life is a team effort and I could not ask for a better husband.

June 2018

Nazmia HUMAIRA
(Control & Aeronautical Engineer)

TABLE OF CONTENTS

Page

ABBREVIATIONS

BVR	**:** Beyond Visual Range
E-M	**:** Energy - Maneuverability
ECM	**:** Electronic Countermeasure
H-M	**:** Altitude - Mach
KE	**:** Kinetic Energy
PE	**:** Potential Energy
ROC	**:** Rate of Climb
TCA	**:** Track Crossing Angle
TSFC	**:** Thrust Specific Fuel Consumption
T/W	**:** Thrust to Weight Ratio
USAF	**:** United States Air Force
USN	**:** United States Navy
WVR	**:** Within Visual Range
W/S	**:** Wing Loading

SYMBOLS

α	: Angle of attack
γ	: Path angle
μ	: Bank angle
γ_s	: Ratio of specific heat (1.4 for air)
ϕ_T	: Angle between thrust line and the body X axis
η_0	: Overall powerplant efficiency
ρ	: Air density
ω	: Turn rate
ω_i	: Instantaneous turn rate
ω_{max}	: Maximum instantaneous turn rate
ω_s	: Sustained turn rate
b	: Wing span
C_{D_0}	: Profile drag coefficient
C_D	: Overall drag coefficient
C_L	: Lift coefficient
$C_{L_{max}}$	: Maximum lift coefficient
D	: Drag force
E	: Total energy of the aircraft
$\mathbf{E_s}$	: Specific energy
$\mathbf{E_{s_i}}$	: Initial specific energy
g	: Gravitational acceleration
h	: Altitude
H_e	: Heat content of the fuel
K	: Aircraft specific constant characteristic
L	: Lift force
n	: Load factor
n_{max}	: Maximum load factor
n_{max_L}	: Lift limited maximum load factor
n_{max_S}	: Structurally limited maximum load factor
n_{min}	: Minimum load factor
m	: Mass
M	: Mach number
P	: Ambient static pressure
P_s	: Specific excess power
q	: Dynamic pressure
R	: Turn radius
S	: Wing surface area
T	: Thrust force
V	: Velocity
V_c	: Corner speed
V_s	: Stall speed
W	: Weight
W_f	: Fuel weight

LIST OF TABLES

Page

LIST OF FIGURES

Page

ENERGY-BASED METRICS FOR FIGHTER AIRCRAFT ASSESSMENT

SUMMARY

Aerial combat is the cornerstone of military operations. One of the seminal elements that determine its outcome is aircraft maneuver. It is not easy to decide how fighter aircrafts will perform in combat, since reliable data regarding them are not usually available. Aircraft manufacturers and air forces frequently assert that their fighters are more superior than other equivalent fighters. However, they do not provide the real capabilities information of their fighters due to confidentiality reason. This study focuses on using existing flight envelopes and energy-maneuverability metrics for fighter aircraft assessment. The flight envelopes will be used to evaluate and compare fighter capabilities while the metrics will be applied to a decision process used to determine the best input strategy for various combat maneuvers.

A fighter aircraft is hardly more superior than its adversary at every altitude and at all speeds. A well experienced pilot knows how to benefit from the weak points of the adversary. He/she may force the adversary at the points where his/her aircraft possesses obvious advantages and launches offensive actions. Pilot, who enjoys and can maintain this advantage, may not only control the combat but also determine its outcome. In this study, three diagrams that can be used to assess aircraft performance and maneuverability during combat will be discussed. They are V-n diagram, Specific Excess Power (P_s) diagram, and Energy-Maneuverability (E-M) diagram. V-n diagram shows the instantaneous maneuvering capability of an aircraft while P_s diagram displays its sustained maneuvering capability. E-M diagram shows both the instantaneous and sustained maneuvering capabilities. Three comparison techniques using these envelopes, will be presented. They are V-n overlay, P_s overlay, and E-M overlay.

The fundamental rules for a successful aerial combat are quick kill, energy management, and assessment of transient characteristics. During combat, pilot must continuously evaluate his/her energy while at the same time assess the energy of the enemy. In an effort to gain energy advantage, both opponents will trade altitude for airspeed or airspeed for altitude many times. Energy should not be expended either too fast or too large. The assessment of aircraft transient characteristics allows us to give a final remark in determining the best input strategy for fighter maneuvers.

SAVAŞ UÇAĞI DEĞERLENDİRMESİ İÇİN ENERJİ TABANLI METRİKLER

ÖZET

Hava savaşı askeri operasyonların temeli haline geldi. Savaş boyunca, uçak manevraları, savaşın sonucunu belirleyen temel faktörlerden biridir. Savaş uçaklarının savaşta nasıl bir performans göstereceğine karar vermek kolay değildir, çünkü bunlarla ilgili güvenilir veriler genellikle mevcut değildir. Uçak üreticileri ve hava kuvvetleri sıklıkla uçaklarının diğer eşdeğer uçaklardan daha üstün olduğunu iddia ediyorlar. Ancak, gizlilik sebebi nedeniyle uçaklarının gerçek yetenek bilgilerini vermezler. Bu tez, savaş uçağı değerlendirmesi için mevcut uçuş zarflarının ve enerji manevra kabiliyet metriklerinin kullanılmasına odaklanmaktadır. Uçuş zarfları, uçağın yeteneklerini değerlendirmek ve karşılaştırmak için kullanılırken, metrikler çeşitli savaş manevraları için en iyi giriş stratejisini belirlemek için kullanılan bir karar sürecine uygulanacaktır.

Bu çalışma bir point-mass uçak modeli kullanmaktadır. Bu modelde, kuvvetlerin ağırlık merkezi üzerinde hareket ettiği varsayılmaktadır. John Boyd ve Thomas Christie tarafından geliştirilen Energy-Maneuverability (E-M) teorisi de uygulanmaktadır. Bu analiz, uçağın kinetik ve potansiyel enerjisinin değişimi, yakıttan enerji ve sürtünme ile yayılan enerji arasındaki dengeyi kullanır. Bilgisayar simülasyonunu kullanmanın yanısıra, bu çalışma Endonezya Ulusal Silahlı Kuvvetleri'nin hava kuvvetleri kolu olan Endonezya Hava Kuvvetleri (TNI AU) F-16 pilotu ile yapılan tartışmaların sonuçlarını içermektedir. Gerçekçi hava muharebesi ve savaş manevraları üzerine birçok bakış açısı verir. Bakış açısı, uçağı değerlendirmesi için uygun karşılaştırma tekniklerinin seçilmesinde ve karar sürecinin yeniden şekillendirilmesinde kullanılır.

Bir savaş uçağı, her irtifada ve her hızda rakiplerinden daha üstün olamaz. İyi tecrübeli bir pilot, rakibin zayıf noktalarından nasıl yararlanacağını bilir. Düşmanını, uçağının bariz avantajlara sahip olduğu noktalarda zorlayabilir ve hücum eylemlerini başlatır. Bu avantajı sahiplenip koruyabilen pilot, sadece savaşı kontrol etmekle kalmayıp, sonucunu da belirleyebilir. Bu çalışmada, savaş sırasında uçak performansını ve manevra kabiliyetini değerlendirmek için kullanılabilecek üç diyagram ele alınacaktır. Bunlar V-n diyagramı, Spesifik Aşırı Güç (P_s) diyagramı, ve Enerji-Manevra kabiliyeti (E-M) diyagramıdır. V-n diyagramı bir uçağın anlık manevra kabiliyetini gösterirken P_s diyagramı sürekli manevra kabiliyetini gösterir. E-M diyagramı hem anlık hem de sürekli manevra kabiliyetlerini gösterir. Bu zarfları kullanan üç karşılaştırma tekniği sunulacaktır. Onlar V-n overlay, P_s overlay, ve E-M overlay.

V-n diyagramı, bir uçağın anlık manevra kabiliyetini göstermektedir. Dikey eksende yük faktörü vardır ve hızı yatay eksendedir. Diyagramın şeklini veren özel koşullar sabit ağırlık, sabit yükseklik, sabit yapılandırma ve sabit itme veya güç seviyesidir. V-n diyagramının sınırları, sol taraftaki maksimum ve minimum taşıma, sağ taraftaki

maksimum dinamik basınç, üst ve alt sınırları ise maksimum ve minimum yük faktörü ile belirlenir.

P_s diyagramı dikey eksende irtifaya ve yatay eksende hıza sahiptir. P_s diyagramının şeklini belirleyen özel koşullar sabit ağırlık, sabit yük faktörü, sabit itme gücü veya güç seviyesi ve sabit yapılandırmadır. Maksimum kararlı durum performansı, bir uçağın çalışma zarfı olarak bilinen $P_s = 0$ kontur ile gösterilir. Zarfın içinde, P_s pozitiftir, yani uçak, hızlanmak, tırmanmak veya her ikisini birden yapmak için yeterli güce sahiptir. Zarfın dışında, P_s negatiftir ve bu nedenle sadece enerji kaybetme pahasına, uçak bu bölgede kısa bir süre uçabilir.

E-M diyagramı dikey eksende dönüş oranına (ω) ve yatay eksende hıza sahiptir. Savaş uçakları için yüksek dönme kabiliyetine sahip olmak önemlidir, çünkü bu yetenek rakiplerine göre daha hızlı atış pozisyonuna ulaşmalarını sağlar. E-M diyagramının şeklini belirleyen özel koşullar sabit ağırlık, sabit yükseklik, sabit itme gücü veya güç seviyesi ve sabit yapılandırmadır. E-M diyagramı üç limite sahiptir: sol tarafta maksimum taşıma, üst tarafta maksimum yük faktörü ve sağ tarafta maksimum dinamik basınç. Enerji kazanma ve kaybetme bölgesinin sınırını işaretlemek için, $P_s = 0$ kontur da verilir. Diyagram, sabit yük faktörü ve dönüş yarıçapı (R) konturları da içerir.

Bu çalışmada, savaş uçağı kabiliyet değerlendirmesinde, P_s, yükleme faktörü, dönüş oranı ve dönüş yarıçapı gibi E-M parametrelerine odaklanmıştır. P_s ve dönüş oranını en üst düzeye çıkarmak ve dönüş yarıçapını aynı anda en aza indirmek mümkün değildir. Yüksek enerji durumunda (yüksek hız ve yüksek P_s), uçak tırmanma, dönme ve hızlanma gibi birçok manevra yapabilir, ancak dönüş oranı azalır ve dönüş yarıçapı artar. Düşük enerji durumunda (düşük hız ve düşük P_s), dönüş yarıçapı azalır ve dönüş oranı artar, oysa uçağın manevra yapması için yeterli enerjiye sahip olmadığından saldırılara karşı savunmasızdır.

Hava savaşında temel noktalar hızlı öldürme ve enerji yönetimidir. Savaş boyunca, pilot genellikle birkaç defansif ve hücumlu manevralar gerçekleştirmek zorundadır. Her manevra, ya kazanılan ya da harcanan enerjiyle sonuçlanır. Düşmana karşı bir enerji avantajı kazanmak ve manevra enerjisinin zamansız kaybını önlemek önemlidir. Ancak, en iyi giriş stratejisini belirlemek sadece manevra süresini ve harcanan enerjiyi analiz ederek yapılamaz. Manevra boyunca yük faktörü, hız, dönüş oranı ve P_s varyasyonu gibi diğer parametreler de dikkate alınmalıdır. Böylece, manevra sırasında zaman, harcanan enerji ve kısıtlama varyasyonlarını değerlendirmek için üç metrik kullanılacaktır: manevra zamanı, enerji çevikliği, ve geçici çeviklik metrikleridir.

Manevra süresi, manevrayı tamamlamak için gereken süreyi ölçer. Enerji-çeviklik metrik parametresi, belirli bir manevrayı tamamlamak için harcanan enerjiyi ölçmek için kullanılır. Genellikle, zaman-enerji eğrisi, başlangıçtaki spesifik enerjinin (E_{s_i}) seviye çizgisinin altındadır. Bunun nedeni enerji genellikle manevra sırasında tüketilmektedir. Sonundaki toplam enerji genellikle manevranın başlangıcındaki toplam enerjiden daha azdır. Fakat, zaman-enerji eğrisinin E_{s_i} çizgisinin üzerinde olduğu birkaç manevra da vardır. Bu durumda, enerji harcanmaz, ancak kazanılır ve sonundaki toplam enerji başlangıçtaki toplam enerjiden daha yüksektir. Böylece, E_{s_i} çizgisi ve zaman-enerji eğrisi arasındaki alanın gölgelenmesi durumunda, bu enerjinin harcanması anlamına gelir. Zaman-enerji eğrisi ile E_{s_i} çizgisi arasındaki alanın gölgelenmesi durumunda, enerjinin kazanıldığını gösterir. Geçici çeviklik metriği P_s, ω, n, V, R ve h gibi parametreleri içerir. Manevra sırasında, uçağın maksimum

ve minimum yük faktörünü, kritik hızını, maksimum hızı ve maksimum dönüş oranı sınırlarını aşmaması önemlidir. Dahası, gelecekteki manevra dizileri için manevranın sonunda dönme kapasitesi (dönüş oranı ve dönüş yarıçapı) da değerlendirilmelidir. Metrik bilginin gösterimi zaman dilimi grafikleri ile elde edilir.

Pilot genellikle, uçağın enerjisini kokpitteki hız göstergesi ve uçağın rakiplerinden göreceli konumu aracılığıyla gözler. Genel olarak, banka açısı ve oranı eğitim prosedürlerine göre belirlenir. Pilot genellikle onların büyüklüklerini bilmek için ADI (Attitude Director Indicator) kullanır. Ancak, yüzlerce uçuş saatinden sonra, ADI kullanmak yerine, pilot banka açısı girişinin büyüklüğünü belirlemek için sezgisini kullanır. Genellikle, pilot düşman uçağının taşıma vektör pozisyonuna dayanarak manevra girişlerini belirler. Bu nedenle, low yo-yo manevrası sırasında banka açısı girişinin büyüklüğü rakibin konumuna ve uçağın taşıma vektörünün istenen yönüne bağlıdır. Eğim açısının ve oranının büyüklükleri için pilotun rakibine göre uçtuğu noktaya bağlı olarak ayarlanır. Bu karar örneğin takip türünü belirleyecektir: lead, lag veya pure. Bu çalışmada, uçak manevraları dikkate alındığında, aileron roll, immelmann, low yo-yo ve high yo-yo gibi bazı temel savaş manevraları bulunmaktadır.

Başarılı bir hava savaşı için temel kurallar hızlı öldürme, enerji yönetimi, ve geçici özelliklerin değerlendirilmesidir. Savaş sırasında, pilot enerjisini sürekli değerlendirmeli ve aynı zamanda düşmanın enerjisini de değerlendirmelidir. Enerji avantajı elde etmek için her iki rakip de hız için irtifayı ya da irtifa için hızı bir çok kez takas edecekler. Bu bilgi başarılı bir savaş için gereklidir. Enerji çok hızlı veya çok büyük bir şekilde harcanmamalıdır. Savaş uçaklarının geçici özelliklerinin değerlendirilmesi, savaş manevraları için en iyi giriş stratejisini belirlemede son bir yorum yapmamızı sağlar.

Tam askeri verilere erişim olmadan, bu çalışmanın sonucunun sadece temsilci olarak kabul edilebileceğine ve bu hesaplamaların diğer sonuçlarının varlığına dair bir ihtimal olduğuna inanılmaktadır. Verileri ikincil kaynaklıdır ve mevcut olan verilerin eksikliğinden dolayı bazı parametreler daha az belirgindir. Yine de, sonuçlar yazarın tahminlerini destekliyor görünmektedir.

Yakın gelecekte, hava savaşını kazanmak için uçağın manevra kabiliyetinin önemi tartışılabilir. Önemli özellik, örneğin uçağın yeteneklerinden füze yeteneğine geçebilir. Füzeler ve radar teknolojisi uçak teknolojisinden daha sık gelişti. Savaşı kazanmak için uçakların sadece yeterli miktarda füze taşımaları, mükemmel radar ve kendini savunma yeteneklerine sahip olmaları gerekir. Hız ve E-M parametrelerinin üstünlüğü dışında, silahlar, menzil kabiliyeti, radar sistemleri (düşmanın tespiti), düşman tarafından tespit edilmekten kaçınma kabiliyeti, havada yakıt ikmali ve pilot kabiliyeti etkinliği belirleyen diğer önemli faktörlerdir. Bu nedenle savaş planlaması boyunca bu parametreler arasında bir denge veya uzlaşma sağlamak için dikkatli bir inceleme yapılmalıdır.

1. INTRODUCTION

1.1 Background

Aerial fight has become a basis of military operations. Throughout combat, aircraft maneuver is one of the key factors that determine its outcome. During World War I and II, sustained maneuvering capability was prominent seeing that fighter aircrafts used the fixed forward firing gun as the first-line air-to-air weapon. Performance levels at fixed points in the flight envelope, such as maximum level speed, maximum engine power, rate of climb, minimum turn radius and maximum turn rate were the measures of merit at that time. In the course of Korean and Vietnam wars, jet fighter aircrafts with growing altitude and Mach ranges and the short range heat seeking missiles came out. These missiles required maneuvers for a stable, rear-aspect firing position. As aircraft capability increased, the measures of merit shifted to advanced point performances such as thrust-to-weight ratio, wing-loading, and energy-maneuverability method [1]. Currently, with the advent of all-aspect missiles, the requirement to maneuver in a very short time-span emerged. Aerial combat strategies have shifted from the requirement to maneuver to reach a stable, rear-aspect firing position into brief, point and shoot maneuvers. Today, aerial combat consists not only of sequences of sustained maneuvers but also sequences of transient maneuvers. In order to evaluate the maneuvering capabilities of fighter aircrafts with the new level of technology, the need of modern performance metrics known as agility metrics arises.

The differences between performance, maneuverability and agility metrics have been discussed in many sources. Performance concerns with the state variables of the aircraft, while maneuverability and agility deal with the first and second time derivatives of aircraft state, respectively [2, 3]. An example of aircraft state is velocity. In this case, performance examines velocity, while maneuverability and agility analyze acceleration and rate of change of acceleration, respectively. Other definitions of maneuverability and agility do exist. Reference [4–6] stated that maneuverability is

the aircraft's capability to change direction and/or magnitude of its velocity vector by turning, accelerating and climbing. Reference [7] described agility as the collaboration of wide sensor coverage, wide weapon-launch envelopes, high acceleration, high maneuverability and short response time required to fight a highly maneuverable enemy. The combination of aircraft, sensor and weapon agility form the system agility. In this study, only aircraft agility will be taken into account. Reference [6] described an aircraft, which is able to perform rapid and accurate changes in flight direction, speed and climb angle as an agile aircraft. Thus, agility is the capability to perform not only quick but also precise changes in motion. Agility contains maneuverability and controllability, with maneuverability is the capability to perform quick motions and controllability is the capability to exactly control the aircraft during such motions.

Great amount of discussions between experts has been carried out in order to find the types of metric that can be applied to measure performance, maneuverability, and agility. Those metrics will not only enable combat capability assessment of an aircraft but also comparison of capability between friendly and enemy fighters. They can be used to create combat techniques or even assist in selecting aircraft for air force use [8]. Performance assessments are usually performed using energy maneuverability diagrams [9]. Colonel John Boyd developed the energy-maneuverability (E-M) theory to measure aircraft's performance by combining parameters such as instantaneous turning capability, sustained turning capability and specific excess power [10]. Maneuverability assessments can be done using metrics such as relative energy state (RES), combat cycle time (CCT), pointing margin, and dynamic speed turn (DST) [11–13]. Agility assessments can be conducted with metrics such as pitch agility, torsional agility, axial agility, roll reversal agility parameter, agility potential, T_{90}, etc. [14]. Brief definition and complete explanation on each can be found in [14] and [15, 16], respectively. In this study, some of existing flight envelopes and metrics will be discussed and used for fighter aircraft assessment. The flight envelopes will be used to evaluate and compare fighter capabilities while the metrics will be applied to a decision process used to determine the best input strategy for various combat maneuvers.

1.2 Methodology

This study uses a point-mass aircraft model, in which forces are assumed to act on the center of gravity of the aircraft. The Energy-Maneuverability (E-M) theory developed by John Boyd and Thomas Christie, is also applied. This analysis makes use of an equilibrium between the changes of aircraft's kinetic and potential energy, energy from fuel, and energy dissipated by drag.

Besides using computer simulation, this study includes the results of discussions with a F-16 pilot from Indonesian Air Force (TNI AU), the air force branch of the Indonesian National Armed Forces. He gives many perspectives on realistic aerial combat and fighter maneuvers. His points of view are used in selecting suitable comparison techniques for fighter assessment and in reshaping the decision process.

1.3 Purpose of Thesis

The main purpose of this thesis is to answer the following questions:

1. What are the flight envelopes and metrics that can be used to measure the combat capability of an aircraft?

2. What is the expected outcome of an aerial combat, under various conditions of parameters (altitude, airspeed, load factor, turn rate, etc.) between an aircraft of a particular design and a given enemy aircraft?

3. What are the metrics that can be used to determine the best input strategy for combat maneuvers?

1.4 Outline of Thesis

Chapter 1 contains introduction, literature review or background for the research. It describes the current state of the topic and the contributions the thesis aims to make in the study of fighter aircraft's combat capability assessment. Chapter 2 explores further the existing aircraft performance, maneuverability and agility metrics presented in the introduction. It also reviews the energy concept, specific energy and specific

excess power parameters that will be extensively used in the next chapters. Chapter 3 discusses envelopes that can be used for fighter capability assessment. Chapter 4 presents capability comparison techniques using Energy-Maneuverability (E-M) method. Chapter 5 discusses a decision process that can be used to select the best input strategy for several combat maneuvers. Chapter 6 ends the thesis with conclusion and recommendations.

2. PERFORMANCE, MANEUVERABILITY & AGILITY ASSESSMENTS

2.1 Theatre of Aerial Combat

Aircraft maneuvers are one of the key factors that determine the result of an aerial fight. Based on interviews with pilots from various fighter aircraft backgrounds, the outcome of an air combat engagement are determined by five factors: the thrust-to-weight ratio, the ability to change attitude relative to the adversary, the ability to change the flight path relative to the adversary, the quickness of these changes and the preciseness of these changes [17]. The pilot's skill to maximize the maneuvering potential of his/her aircraft is also an important factor that dictates the result of an aerial fight [18]. According to [7], the opening conditions, the capabilities and strategies of the enemy pilot and the fighter system performance are the three key elements that control the result of aerial combat. For the pilot, situational awareness, which consists of understanding the current situation, determining the suitable maneuver and implementing the correct commands, is very important. Pilot should be aware of the characteristics, limitations and capabilities of his/her fighter. He/she might only has a few seconds to think, decide and make a move as an offensive action, such as an approaching missile, is detected.

Fighter aircrafts are grouped in terms of generations, which are determined according to the level of speed, weaponries, the capabilities to detect, engage enemy and mask detection by enemy [19]. Taking speed level as an example, the first generation of fighter aircrafts were limited to fly in the subsonic speed level. With further development in engine technology, the second generation can fly up to speed higher than Mach 1 and the third, fourth and fifth generation fighters can fly faster than Mach 2. The development of fighter aircraft as given in [19] is shown in Table 2.1.

As it has been mentioned before, maneuvering capability is a paramount factor during combat. Even a slight difference in maneuverability can determine which aircraft will win the fight [8]. Early combat mode such as in close or Within Visual Range

Table 2.1 : The development of fighter aircraft

Generation	1st	2nd	3rd	4th	4th+	5th
Era	Korea	1955-1965	1965-1975	1975-1995	1995-present	2005-present
Speed	Subsonic	Mach 1+	Mach 1-2+	Mach 1-2+	Mach 1-2+	Mach 1-2+
Weaponry	Gun only	Gun, IR tail aspect missile	Gun, all aspect radar missile	Gun, all aspect IR & radar missile	Gun, all aspect IR & radar missile	Gun, all aspect IR & radar missile
Engage-ment	$\leq 1500ft$	1-3 miles (tail only)	Limited all aspect	All aspect look down	All aspect look down	All aspect look down
Energy and Maneuver-ability	Low energy, high maneuver-ability	Low energy, low maneuver-ability	Low energy, low maneuver-ability	High energy, high maneuver-ability	High energy, high maneuver-ability	High energy, high maneuver-ability
Detection of Enemy Fighter	None	$\geq 10NM$	$\geq 20NM$	$\leq 50NM$	$\geq 100NM$	$\geq 100NM$
Sensor Fusion	None	None	None	None	Limited	Full
Stealth	None	None	None	None	Reduced RCS	Full

(WVR) combat requires maneuvers for a stable, rear-quarter firing advantage. As each fighter attempts to reach rear aspect firing position, extensive period of dogfights are typical [11]. This requirement promoted extended engagements, which make standard or traditional performance measurements beneficial [14]. These parameters are widely known and the well established ones are summarized in [9]. Aircraft's role will affect the required maneuver performance. For example, good acceleration at high altitude and good climb to height qualities are required by aircraft designed for interceptor role with long range missiles. On the other hand, high instantaneous turn rates maneuvering capability will concern aircraft with air combat role [8]. With the development of new technologies, the types of engagement, assessment and measures of merit evolved. For example, with the arrival of all-aspect missiles, the engagement requirement expanded to include transient maneuvering capability. The historical trends in aerial combat and definitions and metrics of performance, maneuverability, and agility are summarized in Table 2.2 and Table 2.3, respectively.

Table 2.2 : Historical trends in aerial combat

Era	WWI & WWII	Korean War	Now
Engagement	Sustained maneuvering	Sustained maneuvering, stable rear-aspect firing position	Sustained, transient maneuvering
Weaponry	Fixed forward firing gun	Rear-aspect missiles	All-aspect missiles
Assessment	Point performance analysis	Advanced point performance analysis	Agility analysis
Measures of Merit	Max speed, max engine power, rate of climb, min turn radius, max turn rate	T/W, W/S, E-M	E-M, agility metrics

Table 2.3 : Performance, maneuverability, and agility

	Performance	Maneuverability	Agility
Definition	Aircraft state variables (e.g. velocity)	First time derivative of performance (e.g. acceleration). The ability to change the direction and/or magnitude of velocity vector and energy state.	Second time derivative of performance (e.g. rate of acceleration). Eidetics: the ability of the entire weapon system to minimize the time delays between target acquisition and target destruction.
Related Metrics	V-n, P_s, and E-M diagrams	Relative Energy State (RES), Combat Cycle Time (CCT), Pointing Margin (PM), Dynamic Speed Turn (DST)	E-M, transient, experimental, operational agilities

2.2 Performance Metrics

Two examples of predominant performance measures of merit are maximum sustained turn rate and maximum instantaneous turn rate. In aerial combats where it is important to point first to shoot, maneuvering using maximum instantaneous turn rate is needed. In order to reach the best of those measures, low wing-loading (W/S) and high thrust-to-weight (T/W) ratio are engineered during fighter aircraft design [11]. Other existing traditional measures of merit are discussed further below.

- Low wing loading (W/S): this parameter is the ratio of aircraft weight to wing area. The unit is force per unit area. W/S varies depending on fuel consumption, release of external stores, variable wing sweep, airfoils and maneuvering flaps or slats. Wing loading can be used to roughly measure the turning capability of a fighter. Fighter with low wing loading will have high maximum lift-to-weight ratio, which leads to high instantaneous turn rate [6, 20]. Larger wing has bigger capability to force the fighter to fly in a direction other than in which it is currently traveling.

- High thrust to weight ratio (T/W): this parameter is calculated with the sea level thrust of the engine(s) and the same weight used to calculate the wing loading parameter [20]. Because thrust is a function of altitude, the ratio available to the pilot at any given altitude is different than the calculated ratio. Aircraft is likely to have more power to make a move and less weight to be moved as W/S decreases and T/W increases [21]. Thrust to weight ratio is a good measure of aircraft's acceleration capability. For example, when the ratio is greater than one, fighter has the ability to accelerate while flying straight up. The ratio of T/W to W/S is defined as agility potential and its values for several aircrafts from the mid-1940 are given in [21].

- Maximum rate of climb: this parameter is usually referred to maximum rate of climb at sea level [20].

- Maximum level Mach number: in general, this parameter refers to the maximum Mach number at sea level and 36,000 feet, which is the beginning of the standard atmosphere tropopause [20].

- Maximum load factor: higher load factor is related to higher turn rate. When an aircraft has higher load factor limit than its adversary, it means that it can maneuver at a level, which is disadvantageous for the adversary.

- Maximum instantaneous turn rate: this is the turn rate achieved at maximum load factor at a given flight condition. This happens at the airspeed referred to as corner airspeed, where the maximum lift limit line and the maximum structural limit line on the V-n diagram intersect [20]. Instantaneous turn rate advantage may offer a shooting opportunity to the pilot but at a cost of losing energy, which will be discussed further at the following sections.

- Maximum sustained turn rate: without losing either altitude or airspeed, this is the maximum turn rate that an aircraft can sustain. When an aircraft possesses sustained turn rate advantage, it may put continual pressure on the enemy and end the engagement with first shoot opportunity.

- Minimum turn radius: small turn radius are only available at low speeds. When aircraft is capable at maneuvering at small turn radius, it has the advantage of keeping visual contact with other aircrafts. As an aircraft is flying within formation, this capability gives easiness to other aircrafts in giving tactical support during combat.

2.2.1 Energy concept

Energy concept plays a very important role during aerial fight. Rutowski as described in [22], stated that the total energy of an aircraft is the combination of its kinetic and potential energy. Its kinetic energy is proportional to its mass and airspeed while its potential energy is proportional to its mass and altitude.

$$E = PE + KE = mgh + \frac{1}{2}mV^2, \tag{2.1}$$

$$E = Wh + \frac{WV^2}{2g} = W(h + \frac{V^2}{2g}) = (\frac{E}{W})W, \tag{2.2}$$

where E is the total energy of the aircraft, PE is potential energy, KE is kinetic energy, m is aircraft's mass, g is gravitational acceleration, h is altitude, V is velocity and aircraft's weight $W = mg$.

Rutowski presented an equation describing the rate of change of the sum of the kinetic and potential energy, which allowed us to calculate the path of minimum fuel and minimum time to change from one combination of altitude and speed to another. Operational maneuverability and efficiency in terms of energy-maneuverability are associated with energy state and energy rate analogies [4]. Energy Maneuverability analysis or E-M was developed by John Boyd, a U.S Air Force fighter pilot, and Thomas Christie, a mathematician, in the early 1960s. Boyd evaluated the F-4 against the MIG-25 and revealed that F-4 was at serious disadvantage compared to MIG-25 and speeded up its replacement. In the late 1960s, his E-M theory was used to establish the prerequisites for the A-10 and F-15. He founded the "Fighter Mafia" and advanced the development of small, low-cost, lightweight fighter, which resulted in F-16 for the USAF and F-18 for US Navy [23].

The first derivative of Equation 2.2 is:

$$dE = Wd(E/W) + (E/W)dW. \tag{2.3}$$

The conservation of energy over a time interval dt between the energy derived from fuel, the energy dissipated against drag and the change in potential and kinetic energy, should be taken into account during aircraft performance assessment [22]. This principle is expressed by the following equation:

$$dE = \eta_0 H_e dW_f - (E/W)dW_f - DVdt, \tag{2.4}$$

where η_0 is the overall powerplant efficiency, H_e is heat content of the fuel, dW_f is change in fuel weight and D is aircraft's drag. The change in fuel weight depicts the change in aircraft's weight as:

$$dW = -dW_f. \tag{2.5}$$

The parameter $\eta_0 H_e$ expresses the useful work of propulsion per amount of fuel, which can be represented by thrust, T and the fuel rate as:

$$\eta_0 H_e = \frac{TV}{dW_f/dt}. \tag{2.6}$$

Substituting Equations 2.5 and 2.6 into Equation 2.4:

$$dE = TVdt + (E/W)dW - DVdt, \tag{2.7}$$

Substituting Equation 2.3 into Equation 2.7:

$$Wd(E/W) = TVdt - DVdt, \tag{2.8}$$

$$\frac{d(E/W)}{dt} = \frac{(T-D)V}{W}, \tag{2.9}$$

which shows that the energy change is given by the excess power and is affected by the change in aircraft's weight.

2.2.2 Specific energy (E_s)

Instead of using the total energy term, in order to be able to assess the acceleration and climbing capabilities of aircrafts with different weights, the specific energy (E_s) term is used. Specific energy (E_s) or energy height is the total energy divided by aircraft's weight. It has the unit of length. The specific energy (E_s) can be expressed as:

$$E_s = \frac{PE + KE}{W} = \frac{mgh + \frac{1}{2}mV^2}{W} = h + \frac{V^2}{2g}. \tag{2.10}$$

The contours of constant E_s on altitude-airspeed grid gives the points of altitude and airspeed combination that will give the same amount of kinetic and potential energies per amount of weight. For supersonic fighters, instead of airspeed, Mach number can be used in the horizontal axis. For true airspeed plot, the shape of lines of constant E_s is parabolic while for Mach number plot, the shape is not exactly parabolic [6]. Figure 2.1 gives an example of E_s representation on altitude-Mach number diagram.

As stated in [24], Rutowski assumed that the transformation of kinetic energy to potential energy along constant energy line by means of a dive or a zoom, may occur instantly. Therefore, time variable does not exist in the diagram. This assumption showed that in theory, aircraft can zoom or dive between any points along constant E_s contour in zero time. As Equation 2.10 suggests, if there is no loss in kinetic energy, E_s indicates the maximum speed achievable if all the potential energy is transformed to kinetic energy. On the other hand, when there is no loss in potential energy, it shows the maximum altitude within reach if all the kinetic energy is transformed to potential energy.

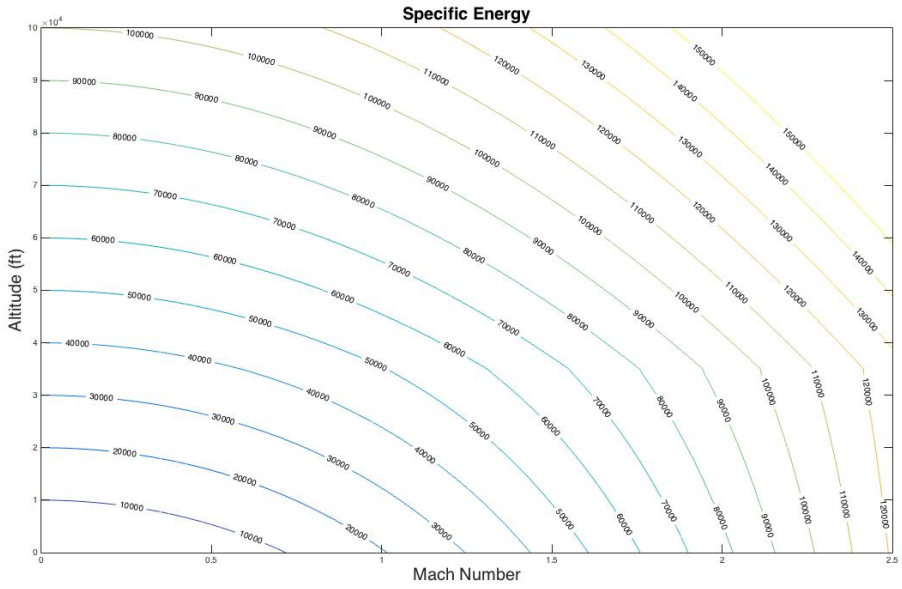

Figure 2.1 : Specific energy diagram

2.2.3 Specific excess power (P_s)

Specific excess power or commonly referred to as P_s, describes fighter's ability to change its energy state. Change in energy or energy rate means power, thus P_s refers to the power accessible to do maneuvers such as climbing, accelerating, decelerating or turning during combat.

$$P_s = \frac{dE_s}{dt}. \tag{2.11}$$

Energy rate is calculated by taking the first derivative of Equation 2.10:

$$\frac{dE_s}{dt} = \frac{dh}{dt} + \frac{V}{g}\frac{dV}{dt}. \tag{2.12}$$

The forces about the aircraft's center of gravity acting parallel to the direction of flight (at zero bank angle) are:

$$T - D - W\sin\gamma = \frac{W}{g}\frac{dV}{dt}, \tag{2.13}$$

where T is thrust, D is drag, and γ is aircraft's flight path angle. Dividing Equation 2.13 with W/V:

$$\frac{V(T-D)}{W} = V\sin\gamma + \frac{V}{g}\frac{dV}{dt}, \tag{2.14}$$

where

$$V\sin\gamma = \frac{dh}{dt}. \tag{2.15}$$

Thus, rewritting Equation 2.14:

$$\frac{V(T-D)}{W} = \frac{dh}{dt} + \frac{V}{g}\frac{dV}{dt}. \tag{2.16}$$

Hence, P_s is:

$$P_s = \frac{V(T-D)}{W}. \tag{2.17}$$

When α (angle of attack) and ϕ_T (angle between thrust line and the body X axis) parameters shall be incorporated, P_s can be expressed as:

$$P_s = \frac{V(T\cos(\alpha-\phi_T)-D)}{W}. \tag{2.18}$$

In terms of T/W and W/S, Reference [8] expresses P_s as:

$$P_s = V\left(\frac{T}{W} - \frac{qC_{D_0}}{W/S} - \frac{Kn^2}{q}\frac{W}{S}\right), \tag{2.19}$$

where it shows that in terms of specific excess power, having high T/W ratio is advantageous. However, with regard to wing loading or W/S, it is not that straightforward. High W/S is advantageous at high speeds (high q) as it reduces the profile drag term ($\frac{qC_{D_0}}{W/S}$), but it is unfavorable at low speeds (low q) and high n as it increases the induced drag term ($\frac{Kn^2}{q}\frac{W}{S}$).

Equation 2.16 contains terms for both rate of climb and acceleration. Therefore, in the event that aircraft performs level acceleration at constant altitude ($\frac{dh}{dt} = 0$) or climbing at constant airspeed ($\frac{dV}{dt} = 0$), P_s can be used to calculate the corresponding value of acceleration and rate of climb, respectively. P_s has the unit of distance per unit time such as ft/s and ft/min.

From Equation 2.17 and Equation 2.18, it can be seen that P_s gives the remaining power available to do maneuvers after the power dissipated by drag per unit of time is subtracted from the power available to do work per unit of time. According to the maneuver the aircraft is doing, several parameters determine the magnitudes of thrust available and thrust required. For example, during level turn, thrust available depends on Mach number, altitude and ambient temperature while thrust required depends on Mach number and weight [6]. Unlike turboprop or piston aircrafts, the thrust of military power turbojet aircraft is independent of airspeed [24]. The thrust required and thrust available curves multiplied by the velocity can be used to obtain the power required and power available curves.

Table 2.4 : P_s at level flight & during climbing

P_s sign	ROC sign	Aircraft's instantaneous dynamic condition
P_s>0	ROC=0	Aircraft accelerates
P_s>0	ROC>0	Aircraft climbs
P_s<0	ROC=0	Aircraft decelerates
P_s<0	ROC<0	Aircraft descends
P_s=0	ROC=0	Aircraft flies at constant speed at level flight

From the magnitude and sign of P_s, the instantaneous dynamic condition of the aircraft can be analyzed. Positive P_s indicates positive energy rate, which means that energy is gained. Its magnitude becomes a measure of rate of climb at constant velocity, acceleration at constant altitude or combination of climb and acceleration. On the contrary, negative P_s signifies negative energy rate, which means that energy is lost. It becomes a measure of loss of altitude, deceleration or both. When thrust and drag are equal, P_s is zero. This refers to a steady-state condition where airplane is neither accelerating nor decelerating. It is important to note that when $P_s = 0$, aircraft still can accelerate but it will need to descend simultaneously and it still can climb but its forward speed will decrease. For an aircraft flying at fixed thrust and fixed forward speed, in terms of level flight and climb performance, P_s can be assessed as shown in Table 2.4.

2.3 Maneuverability Metrics

2.3.1 Ponting margin (PM)

Introduced by [11], pointing margin (PM) evaluates fighter aircrafts first-shoot capability or the capability to point quickly at an adversary during combat. It measures the angle between the nose of the adversary and the line of sight of the friendly fighter. The maneuver starts at the time both the adversary and friendly aircrafts begin maximum instantaneous turn rate turns and the maneuver ends when one aircraft is able to point its weapon to the other. By continuing to turn until PM is zero, the adversary may also shoot its weapon. The time it takes for the adversary to do this is called the time-pointing-margin. If the friendly fighter missile time of flight is lower than the adversary time-pointing margin, the friendly can destroy the adversary before it launches its weapon. Otherwise, mutual hit scenario is possible. The drawbacks of

using this metric are that it does not take into account energy and it greatly depends on the adversary maneuvers. In the case the friendly fails to shoot down the adversary, it will be in a vulnerable low energy state.

2.3.2 Combat cycle time (CCT)

Established by [11], combat cycle time (CCT) is a combination of maneuvers superimposed on the E-M diagram. It measures the total time needed to perform a 180 degree heading change and return to the original energy state.

$$CCT = t_1 + t_2 + t_3 + t_4 \tag{2.20}$$

where t_1= pitch up to load factor limit, t_2= turn along load factor and lift limit, t_3= unload from elevated angle of attack/load factor and t_4= regain original energy level. Unlike the PM metric, CCT does not take into account firing opportunity.

2.3.3 Relative energy state (RES)

Even though first-shoot capability is crucial as we have seen depicted in PM metric, aerial combat does not only consist of first-shoot maneuver. If the friendly fails to shoot down the adversary in the first-shoot phenomenon, it will suffer from great amount of energy loss and degraded maneuverability. In combat counting in more than two participants, it is important to avoid untimely loss of maneuvering energy. Taking this into consideration, [11] proposed the relative energy state (RES) metric, which measures the energy efficiency of aircraft during combat. RES metric requires that at least two 90 degree turns must be done before the speed of the aircraft falls below the corner speed [1]. Corner speed (V_c) is a paramount parameter during aerial combat. At that speed, aircraft has its highest turn rate and lowest turn radius. Speed below V_c shows that aircraft has consumed its maneuvering potential in order to maximize its pointing capability, whereas speed above V_c suggests that aircraft has not maximized its pointing capability and keeps its energy for future maneuvers.

2.3.4 Dynamic speed turn (DST)

E-M analysis measures only the steady state performance of an aircraft in a highly dynamic situation of aerial combat. Taking this drawback into consideration, [12] developed the dynamic speed turn (DST) metric from the E-M diagram introduced

by [4]. DST integrates the dynamics of turning and accelerating over a wide range of airspeed and the capability of nose pointing, continue pointing, disengage and regaining speed [1]. For each point along the maneuver limit line and for each point along the 1 g maneuver line of E-M diagram, the turn rate vs bleed rate and the acceleration vs airspeed plots are created, respectively.

2.3.5 Kutschera metric

In the conclusion part of their final report, [15] stated that developing a metric that combine energy efficiency, maneuver time and turn radius into one parameter would be very beneficial. Taking this into account, [13] proposed a metric, which combines four parameters to quantify aircraft performance. Those four parameters are the time taken to complete the maneuver, the final P_s at the end of the maneuver, the energy change throughout the maneuver and the turn diameter.

2.4 Agility Metrics

Other than maneuverability, weaponry, low observability, speed, acceleration, payload and range performance, agility is also an important feature in aerial combat. According to [17], there are two reasons that drive the necessity to define and quantify agility. They are the deficiencies of the traditional performance metrics to measure the aircraft transient performance and to assess the advanced aircraft technologies and capabilities such as high angle of attack flight controls and thrust vectoring and reversing. A more agile aircraft is an aircraft, which is capable of doing more state-change activities in less time than its adversary [25]. These activities are classified into instantaneous, SAT (Small Amplitude Task), and LAT (Large Amplitude Task). The elements of aircraft agility are flight path change, quickness, attitude change and precision and the metrics are categorized into nose pointing agility (pitch and yaw pointing) and flight path agility (axial, pitch, roll) [17]. Reference [26] gave varying definitions of agility given by a number of experts, in which all agree that agility relates to the ability of an aircraft to reach desired requirement in a minimum time. A more complete illustration of the relative air combat capability with a combination of torsional agility and E-M analysis comparisons are also given.

Table 2.5 : AGARD airframe agility metrics classification

Metric Class	**Defined by**	**Measure**
Transient	Flight mechanic characteristics regardless of the maneuver	Physical property of the response
Experimental	Completion of a small task (translational, nose pointing & torsional)	Compound property
Operational	Completion of a mission task element (MTE)	Time for completion, precision and aggressiveness

Reference [14, 15] classified agility metrics into two categories: based on the axis in which the maneuvers are carried out and based on the timescale of the maneuver. In the first category, there are three classes: axial, longitudinal and lateral. In the second one, there are also three classes: transient, functional and potential. The metrics categorization into longitudinal, torsional and axial depending on the maneuver axis is also given in [27]. Reference [26] gave two specific agility areas that need to be addressed based on multiple surveys performed since 1984 with USAF and U.S. Navy Fighter Weapon School instructors and operational pilots. They are the difference in the capabilities of two conflicting aircraft to roll while executing a high angle of attack turning maneuver and the capability of an aircraft to pitch down from a high load factor maneuver at high angle of attack/high drag to an unloaded, low angle of attack/low drag condition to accelerate to a higher airspeed. This study prefers the categorization of agility given in [16]. There, agility is classified into transient, experimental and operational, as shown in Table 2.5.

2.4.1 Transient agility metric

The transient agility metrics describe the continuous characteristics of transient response regardless of the maneuver choice. Several metric titles and parameters are given. Nevertheless, only the energy-maneuverability with its corresponding P_s, ω, n metric parameters, which satisfy all the attribute codes. This fact supports the author's assumption that the traditional performance measures of merit still can be used to assess the agility of modern fighter aircrafts.

2.4.2 Experimental agility metric

The experimental agility metrics represent the specific building blocks of the motion commanded by the pilot. They may be divided into pure translational (forward, sidewards or vertical translation of aircraft center of gravity), nose pointing (change of body axis orientation with respect to the velocity vector or direction of lift/maneuver plane), and torsional (lift/maneuver plane rotation about the velocity vector). Axial acceleration, which is represented in terms of P_s, is one example of translational metrics. In the nose pointing metric class, there is instantaneous turn rates, similar to E-M plot by Boyd. In torsional metric class, one example is peak roll rate.

2.4.3 Operational agility metric

Operational agility metrics consider the performance, maneuvering and man-machine interface aspects of aircraft agility. Their two objectives are mission task quickness and mission task precision. The global operational agility metrics are the time to perform a mission task element (MTE), energy agility and aiming error. The fighter operational agility metrics are pointing margin (PM), relative energy state (RES), dynamic speed turn (DST) and combat cycle time (CCT).

3. AIRCRAFT FLIGHT ENVELOPES

Aircraft's flight envelope, determined by its mission requirements, is the airspace in which aircraft is constrained to fly [23]. As cited from Ruijgrok, the traditional definition of aircraft's flight envelope is a diagram, which shows the ranges of altitude and airspeed in which aircraft is allowed to fly [28]. In this study, three diagrams that can be used to assess aircraft performance and maneuverability during combat will be discussed. They are V-n diagram, Specific Excess Power (P_s) diagram, and Energy-Maneuverability (E-M) diagram. E-M diagram is also known as doghouse diagram. The interacting energy connections that are fundamental to energy-maneuverability theory, are procured by using V-n diagram and H-M diagram [4]. In this study, H-M diagram is referred to as P_s diagram.

V-n diagram shows the instantaneous maneuvering capability of an aircraft while P_s diagram displays its sustained maneuvering capability. E-M diagram shows both the instantaneous and sustained maneuvering capabilities. Instantaneous capability means the maneuver that an aircraft can perform in an instant or for a very short time while afterwards the performance of the aircraft may degrade straightaway [29]. On the contrary, sustained capability means the maneuver that an aircraft is capable to perform for a long period of time. P_s diagram can be applied mainly for vertical plane analysis while E-M diagram can be used for horizontal plane analysis for example, during level turn. Operational maneuverability and efficiency of varying weapon, engine, and airframe combinations are shown by these diagrams.

3.1 Limitations

There are several restrictions that determine the boundaries of aircraft flight envelopes. They are for example stall, buffet, controllability, structural, dynamic pressure, sonic boom, thrust, and temperature limitations. They arise due to several factors such as airframe, engine, comfort, and environmental requirements. The intersection of those

limitations form flight envelope, which is defined as the area where aircraft can fly safely. Details on those limitations are discussed further below.

- Stall and buffet limits: stall is an event where lift disappears from the wing as a result of abrupt separation of flow from the wing upper surface [23]. Stall limit arises due to $C_{L_{max}}$ or the maximum lift that the aircraft can produce due to aerodynamic stall, pitch up or maximum control deflections [6, 24, 29]. Therefore, it is also known as aircraft's lift limit. It is independent of the atmosphere and flight trajectory and depends only on the shape of the aircraft's wing. Stall speed (V_s) is located along this limit. Below the stall speed, loss of control may occur due to the sudden lost of of lift. The stall speed formula is given by:

$$V_{stall} = \sqrt{\frac{2nW}{\rho S C_{L_{max}}}}, \tag{3.1}$$

  where W is aircraft's weight, n is load factor, ρ is air density, S is wing surface area and $C_{L_{max}}$ is maximum lift coefficient. n is aircraft's load factor, which can be calculated by:

$$n = \frac{L}{W}. \tag{3.2}$$

  Buffeting is a phenomenon where some parts of the aircraft (such as wing or horizontal tail) oscillate irregularly due to turbulence of the airflow separation. For example, in the transonic region, shock waves built up on the wing and the resulting separated flow travels to the horizontal tail and causes it to oscillate irregularly. It comes before stall and is more observable at high speeds. Data on the maximum operational C_L versus Mach number is required to form the stall and buffet boundaries. The maximum C_L is in general near to $C_{L_{max}}$ at low speeds. Nevertheless, as speed increases, the maximum operational C_L decreases and in the transonic region it may fall to one-half or one-third of its $C_{L_{max}}$ at low speed. Therefore, buffeting limits the allowable value of $C_{L_{max}}$ [23].

- Controllability limit: in [5], controllability limit is included in one of its maneuvering diagram but no further discussion concerning this limit is given. According to [6], controllability is the capability to control the flight path during maneuvers. Controllability examines aircraft control surfaces, their deflections and the ability of the pilot in dealing with them.

- Structural limit: structural limit is a constraint in general posed by aircraft's structural strength. In the course of flight envelope discussion, this limit is generally represented by the load factor parameter. As load factor increases, the instantaneous turning capability increases with speed [6]. Below the corner speed, the load factor is limited by $C_{L_{max}}$ while above the corner speed, it is limited by the aircraft's structural strength. The value of this limit also depends on pilot effectiveness in dealing with high load factor environment. Excessive g-loading may lead to some problems for pilot such as, g-induced loss of situational awareness and g-induced loss of consciousness. In order to allow pilot to use the full maneuvering potential of the aircraft, new anti-g flight equipment is built to avoid those problems.

  The higher the allowable load factor, the heavier the weight of the airplane's structure will be. To obtain an aircraft's limit load, its maximum load factor should be multiplied by its weight. Generally, an aircraft can survive its limit load without yielding. The ultimate load factor, the load factor where structural deformation and permanent damage to the structure may arise is about 1.5 times the limit load factor [24]. An aircraft's ultimate load is obtained by multiplying its ultimate load factor by its weight. In general, aircraft is designed to endure the ultimate load without breaking.

- Maximum dynamic pressure limit: aircraft's dynamic pressure (q) is given by:

$$q = \frac{1}{2}\rho V^2 = \frac{\gamma_s}{2} P M^2, \tag{3.3}$$

  where γ_s is the ratio of specific heats (1.4 for air), P is ambient static pressure and M is Mach number. Maximum q limit of present aircrafts is around $2,090 lbs/ft^2$ or $100,000 N/m^2$ [23]. With this limitation, aircraft is not allowed to fly at high supersonic speeds at low altitudes. In the military specification, having a high q limit is advantageous in increasing survivability. High q limit allows friendly fighter to escape early radar detection and sneak into adversary's defense at low altitude and high speed. Adversary fighter with low q limit will not be able to fly at that region. Nevertheless, propulsion, structural weight and hence take off weight of a high q aircraft will obviously increase, which will in turn reduce its performance [23].

- Sonic boom: as aircraft flies at low altitude and/or high Mach number, pressure waves generated on the ground may cause an event known as ground overpressure. Sound like an explosive can be observed as these waves reach the ground. This event can produce harm and inconvenience such as, clattering of window panes and vibrations of buildings. The shape and size of the aircraft, its flight altitude and the atmospheric conditions determine the intensity of the event. As the altitude of the flight decreases, its intensity increases while as the size of the aircraft decreases, it decreases. Therefore, minimum altitude at which an aircraft can fly at high Mach number must be controlled [23].

- Maximum thrust limit: the measures of merit for propulsion system are its thrust specific fuel consumption (TSFC) and thrust per engine weight (T/W) [23, 29]. TSFC is the ratio of rate of fuel consumption to thrust output. Well qualified engines are engines that have high T/W ratio and low TSFC in the regions where aircraft is designed to operate [29]. When the flight envelope of the aircraft is presented with airspeed in the x-axis and altitude in the y-axis, engine's maximum thrust form the boundaries of the top and part of the right side of the envelope. It determines the absolute ceiling or the maximum altitude that the aircraft can achieve. Aircraft's weight and external store configuration also affect the position of this limit line [23].

- Temperature limit: at high speeds, because of conversion of air kinetic energy into thermal energy, the temperature at the surface of the aircraft increases. Depending on the materials used, the temperature limit of aircraft's skin will vary. This limit will also restrict the maximum allowable velocity or Mach number.

- Environmental limitations: environmental limitations arise due to the environment where the aircraft operates. Noise and pollution are two examples of them [23].

Environmental limitations usually concern commercial passenger aircrafts. Since this study is about fighter aircraft assessment, none of that type of limitation will be included. Without access to complete military data and due to the incompleteness of the data available, only some of the limitations explained above will be included in the envelopes. They are stall, structural, maximum dynamic pressure and maximum thrust limits.

3.2 V-n Diagram

V-n or velocity-load factor diagram shows the instantaneous maneuvering capability of an aircraft. It shows the correlation of aircraft's velocity, maneuvering capability and structural strength. It displays the maximum available instantaneous turning performance in terms of available load factor [24]. It has load factor (n) in g unit in the vertical axis and airspeed in the horizontal axis. The important parameters shown on the diagram are corner speed and maximum maneuver limitations such as stall, structural (load factor) and speed. The specific conditions that determine the boundaries of V-n diagram are constant weight, constant altitude, fixed configuration and fixed thrust or power level.

The parameters that determine the boundaries of V-n diagram are lift/stall, structural and maximum speed limits. At low speeds, on the left hand side of the diagram, it is limited by $C_{L_{max}}$ or the maximum lift that the aircraft can produce. The parabolic shape of the lift boundary is due to the fact that lift is proportional to dynamic pressure, q, which is proportional to the speed squared, V^2. Stall speed (V_s), given in Equation 3.1, is located along this limit. Below the stall speed, loss of control may occur due to the sudden lost of of lift. On the right hand side, the limit value may be determined by several factors such as Mach number limit (controllability), dynamic pressure limit (structural strength) or temperature limit (heat generated at high speeds) [29]. In many cases, it is either the maximum speed or the maximum dynamic pressure (q) of the aircraft, which is plotted. In this study, a maximum q limit of $2,090 lbs/ft^2$ or $100,000 N/m^2$ as given in [23] is used. The structural limit of the aircraft is given in the upper and lower boundaries of the diagram. It shows the aircraft's limit load factor due to its materials. The airspeed where the maximum lift limit line and the maximum structural limit line on the V-n diagram intersect indicates a paramount parameter in fighter performance known as the corner speed (V_c). The maximum instantaneous turning capability with maximum rate of turn and minimum turn radius occurs at this speed. The corner speed formulation can be written by substituting the fighter's

maximum load factor (n_{max}) into Equation 3.1:

$$V_c = \sqrt{\frac{2n_{max}W}{\rho S C_{L_{max}}}}. \tag{3.4}$$

An example of a schematic V-n diagram is given in Figure 3.1. Furthermore, Figure 3.2 shows another version of this diagram with Mach number in the x-axis and contours of P_s (rose), turn rate (blue), and turn radius (green) included. One of the disadvantages of V-n diagram is that it is valid only for aircraft doing coordinated turn at a constant airspeed and altitude. As altitude, configuration, thrust level and weight vary, the diagram changes in shape. V-n diagram also does not give any information regarding aircraft's capability of gaining or losing energy due to the lack of thrust and drag information. Fortunately, the P_s diagram, which will be discussed in the following section, can fulfill the need for information on that subject.

3.3 P_s Diagram

Energy maneuverability in terms of P_s has been one of the primary tools not only to show, but also to evaluate and compare the performance capability of a fighter. The graphical tool that can be used for this objective is known as specific excess power plot or P_s diagram. It displays fighter's capability to accelerate, climb and perform stabilized flight [24]. P_s diagram has altitude in the vertical axis and Mach number or airspeed in the horizontal axis. It is useful especially for fighter climb (vertical plane) performance assessment [5]. P_s is highest at sea-level at aircraft's critical Mach number, where thrust is high and drag is low. As altitude increases, P_s shifts and decreases in magnitude. A fighter's combat ceiling, service ceiling and absolute ceiling are the highest point on its $P_s = 500 ft/min$, $P_s = 100 ft/min$ and $P_s = 0$ contours, respectively [24, 29]. The important parameters shown on P_s diagram are sustained maneuver line ($P_s = 0$) and energy gained and lost for any speed and altitude. The specific conditions that determine the boundaries of P_s diagram are constant weight, constant load factor, fixed thrust or power level and fixed configuration. In this diagram, it is assumed that potential and kinetic energy can be exchanged instantaneously and with no losses.

The maximum steady state performance is shown by the $P_s = 0$ contour. The $P_s = 0$ contour is also known as the operating envelope of an aircraft [29]. It shows the

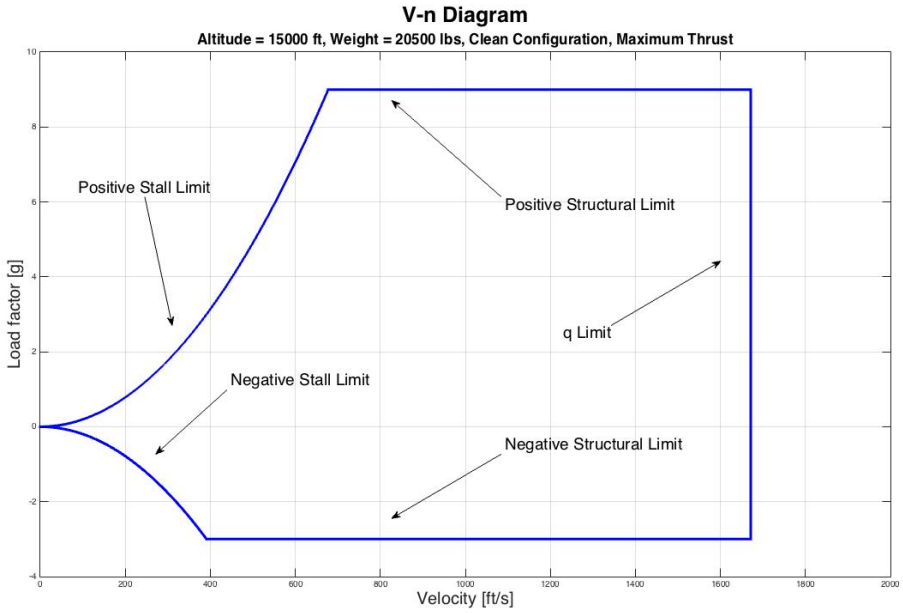

Figure 3.1 : V-n diagram

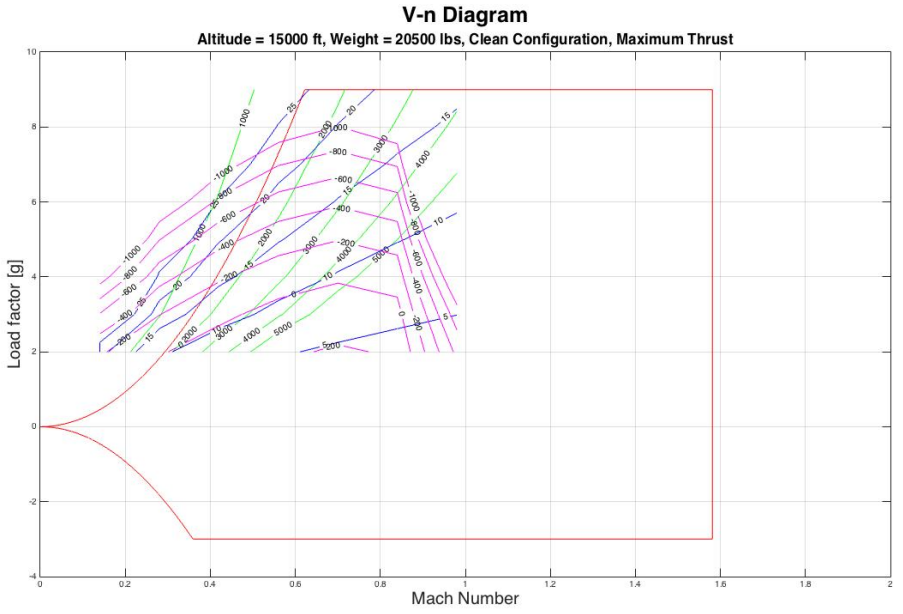

Figure 3.2 : V-n diagram with P_s, n, and R contours

range of airspeed acceptable at different altitudes. Inside the envelope, P_s is positive, thus aircraft has enough thrust to accelerate, climb or both at the same energy state. Inside the operating envelope, advantageous zones or areas for specific combat roles can be determined. For example, the area at the bottom right of the envelope can be marked as advantageous for ground attack fighters since it is important for fighters with that role to fly at high speeds and low altitudes. For interceptor role, where fighter is required to fly at high speeds and high altitudes, the area at the top right of the envelope is advantageous. Outside the $P_s = 0$ contour, P_s is negative and aircraft can not stabilize. As aircraft is flying at a speed and altitude combination that is located in that region, it cannot accelerate without losing altitude or it cannot climb without decelerating/losing airspeed as long as weight, thrust, configuration and load factor do not change. Consequently, only at the expense of losing energy, aircraft can fly for a short period of time outside the envelope.

One of two disadvantages of P_s diagram is that it does not give any information on how long the combatant can preserve his/her P_s advantage as the flight conditions change. Furthermore, it displays only the thrust and airframe capabilities and limitations during maneuver. It does not show other limitations such as structural, aerodynamic, controllability, dynamic pressure and temperature, which also constrain fighter performance. Therefore, it is useful to incorporate for example, the stall boundary on the left hand side of the diagram and the maximum speed or dynamic pressure boundary on the right hand side of the diagram. An example of a schematic P_s diagram of a fighter aircraft is given in Figure 3.3. Rose and red contours indicate the $P_s = 0$ and stall limit contours, respectively. Since P_s diagram is determined for specific conditions of weight, thrust, configuration and load factor, thus, as one of those conditions varies, the diagram will change in shape. An example is shown in Figure 3.4. As load factor increases to $n = 3$, the diagram previously given in Figure 3.3 shrinks and deforms. This is due to the fact that to generate $n = 3$, more induced drag is prompted and more power is required to produce three times greater lift than before.

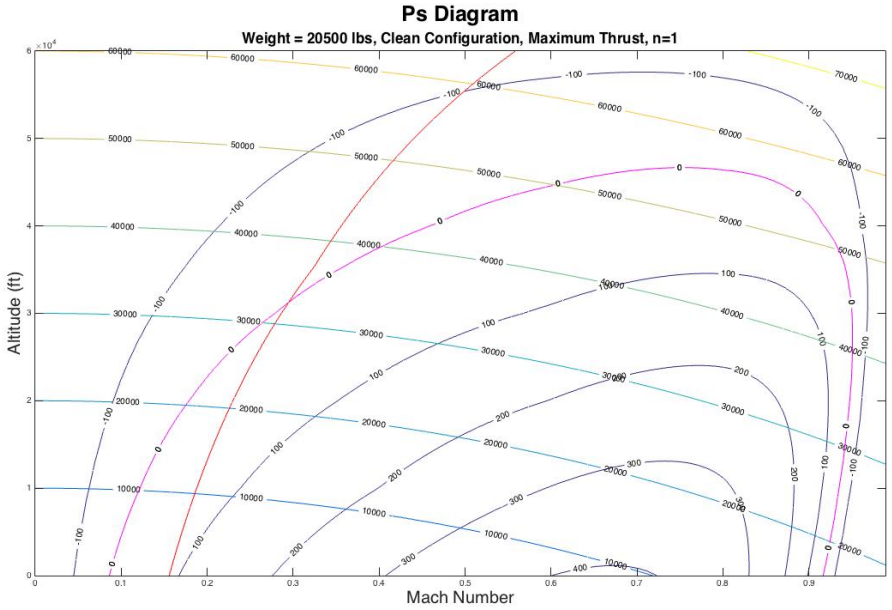

Figure 3.3 : P_s diagram

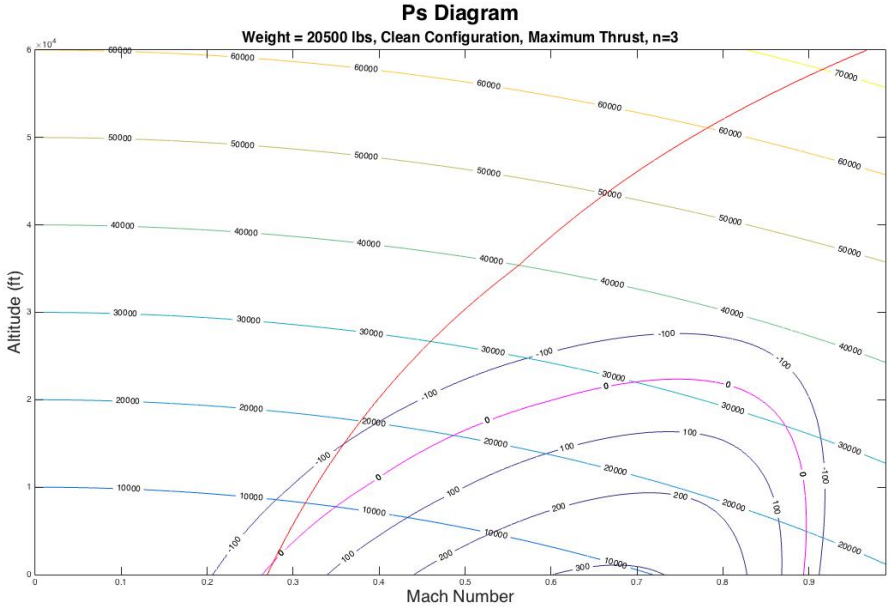

Figure 3.4 : P_s diagram for $n = 3$

3.4 E-M Diagram

E-M diagram is the combination of V-n and P_s diagrams, which displays both the instantaneous and sustained maneuvering capabilities of an aircraft [6, 29]. It is a very important tool in describing and comparing aircraft capabilities. E-M diagram shows the variation of turn rate (ω) with velocity. Turn rate is the angular rate of change of velocity vector, which in general has the unit of degrees/second [5]. The important parameters shown on the diagram are corner speed, turn rate for any speed and load factor, maximum maneuver limits (stall, structural and speed), sustained maneuver line ($P_s = 0$), and energy gained and lost for any speed and turn rate. The specific conditions that determine the boundaries of E-M diagram are constant weight, constant altitude, fixed thrust or power level and fixed configuration.

Similar to P_s diagram, in the E-M diagram, it is assumed that potential and kinetic energy can be exchanged instantaneously and with no losses. E-M diagram has three limits: lift limit, load factor limit and dynamic pressure limit. The lift limit line is located on the left hand side up to the load factor limit line. It indicates the maximum aerodynamic performance of the aircraft. On the top of the diagram, the load factor limit line descends from top left to lower right. The dynamic pressure limit line is found on the right hand side of the diagram. It is useful to incorporate P_s contours into E-M diagram. Generally, it is the $P_s = 0$ contour that is drawn to mark the boundary of the region of gaining energy (positive P_s) and the region of losing energy (negative P_s).

Turn rate is sensitive to airspeed and altitude, which are two elements that constitute aircraft's specific energy. Turning in the horizontal, vertical and oblique planes are produced by the radial acceleration, which is generated from thrust, drag, lift and weight forces. Turn rate (ω) can be calculated using the following equation:

$$\omega = \frac{g}{V}\sqrt{n^2 - 1} = \frac{g}{V}\sqrt{\left(\frac{C_L \rho S V^2}{2W}\right)^2 - 1}. \tag{3.5}$$

Recall that n is load factor, which is given in Equation 3.2. If the turn is performed by tilting the lift vector from the vertical axis, n can also be expressed as a function of bank angle (ϕ):

$$n = \frac{1}{\cos\phi}. \tag{3.6}$$

The lift limited maximum load factor (n_{max_L}) can be expressed as:

$$n_{max_L} = \frac{C_{L_{max}} \rho S V^2}{2W} = \frac{C_{L_{max}} q}{W/S}. \tag{3.7}$$

The structurally limited maximum load factor (n_{max_S}) is usually taken as a constant. In this study, $n_{max_S} = 9$. The maximum load factor (n_{max}) is the minimum of n_{max_L} and n_{max_S}. Hence, the maximum instantaneous turn rate is given as:

$$\omega_{max} = \frac{g}{V} \sqrt{n_{max}^2 - 1}. \tag{3.8}$$

Lines of constant load factor and turn radius (R) can also be plotted on the diagram. Lines of constant turn radius go from lower left to upper right while lines of constant load factor curve down from top left to lower right. Lines of constant turn radius can be calculated by:

$$R = \frac{V^2}{g\sqrt{n^2 - 1}} = \frac{V}{\omega}. \tag{3.9}$$

Lines of constant load factor can be calculated by rearranging Equation 3.5 to solve for n:

$$n = \sqrt{\left(\frac{\omega V}{g}\right)^2 + 1}. \tag{3.10}$$

No turning can be made at 1 g stall speed, since at that speed turn rate is zero and turn radius is infinite [6]. Having a high turning rate capability is important for pilots as that capability allows them to reach firing position faster than their opponents. The instantaneous turn rate (ω_i) and sustained turn rate (ω_s) lines are two important parameters given in the diagram. ω_i shows the highest available turn rate for a given flight conditions [5, 8]. It is determined by the structural strength and the lift capability of the aircraft [6]. Maximum ω_i occurs at the speed referred to as corner speed, where the maximum lift line and the maximum structural limit line intersect. At the corner speed (V_c), aircraft has its maximum turn rate and its minimum turn radius. It is the lowest speed at which maximum structural load factor is feasible. At speeds above V_c, at the maximum load factor line, both turn rate and turn radius suffer. Turn rate decreases and turn radius increases independent of altitude as aircraft is limited by its structural strength. At speeds below V_c and higher altitudes, due to the reduced lift capability, lower turn rates and larger turn radius can also be observed.

As P_s contours are plotted inside the diagram, the turning performance capability of the aircraft can be assessed further. On the ω_s envelope, thrust is equal to drag or $P_s = 0$.

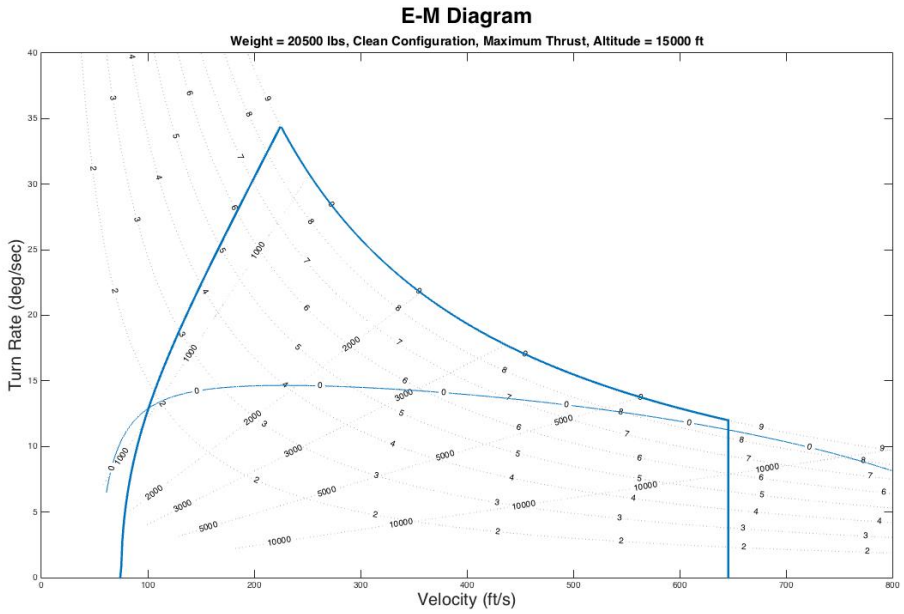

Figure 3.5 : E-M diagram

Inside the ω_s envelope, $P_s > 0$, which means that aircraft can maneuver without losing altitude or decelerating. Above the ω_s envelope, $P_s < 0$, which indicates that aircraft is slowing down and/or losing altitude. The ω_i envelope is usually located above the ω_s envelope and it means that aircraft maneuvering on the ω_i contour is always decelerating or losing altitude. This also shows that ω_i, which defines the maximum turning capability of the aircraft, does not necessarily occur at the highest energy level. During combat, ending a maneuver at a low energy state can trouble the aircraft and pilot may have restricted alternatives for further maneuvers [8]. The disadvantages of E-M diagram are that it does not give any information on how long pilot can perform the instantaneous maneuver and how long he/she can maintain the aircraft's P_s advantage as the flight conditions change. Therefore, careful energy examination and management to achieve a balance or compromise between maneuverability and survivability should be done throughout combat planning. An example of a schematic E-M diagram is given in Figure 3.5.

4. COMPARISON TECHNIQUES

In [18], the difference between energy management and energy maneuverability is given. Energy management refers to the utilization of kinetic, potential and fuel energies to maximize the use of weaponries to fulfill the required task. Energy maneuverability is the analysis of the capacity of the aircraft to change its direction, airspeed and altitude, showed in terms of energy and energy rate. In short, it evaluates aircraft's capability to change its energy state [23]. Designer, planner, tactician and commander may use the energy-maneuverability theory for aircraft performance optimization [4]. Almost always, the best chance of surviving belongs to the aircraft with the highest energy level [8]. Higher energy level shows that fighter has greater capability to maneuver than its enemy. In combat counting in more than two participants, several defensive and offensive maneuvers are required and thus, it is important to avoid untimely loss of maneuvering energy.

In the development of combat strategy, the energy maneuvering capability of one own's fighter should be compared with the maneuvering capability of an enemy's fighter. A fighter aircraft is rarely more superior than its adversary at every altitude and at all speeds. Pilot should know how to take advantage from the weak points of the enemy. This information is necessary for a successful fight. With this information, pilot may force the enemy aircraft for example, to fly in a region where it has higher maneuvering capability and launches offensive actions. When pilot can maintain this advantage, he/she may not only control the combat but also determine its outcome. In this study, three comparison techniques using the flight envelopes that have been discussed before, will be presented. They are V-n overlay, P_s overlay, and E-M overlay.

4.1 V-n Overlay

V-n diagram provides information in a visually accessible, dense and systematic form [5]. A pilot can decide whether he/she has a turn advantage over an adversary or not by overlaying and comparing his/her own V-n diagram with the V-n diagram of

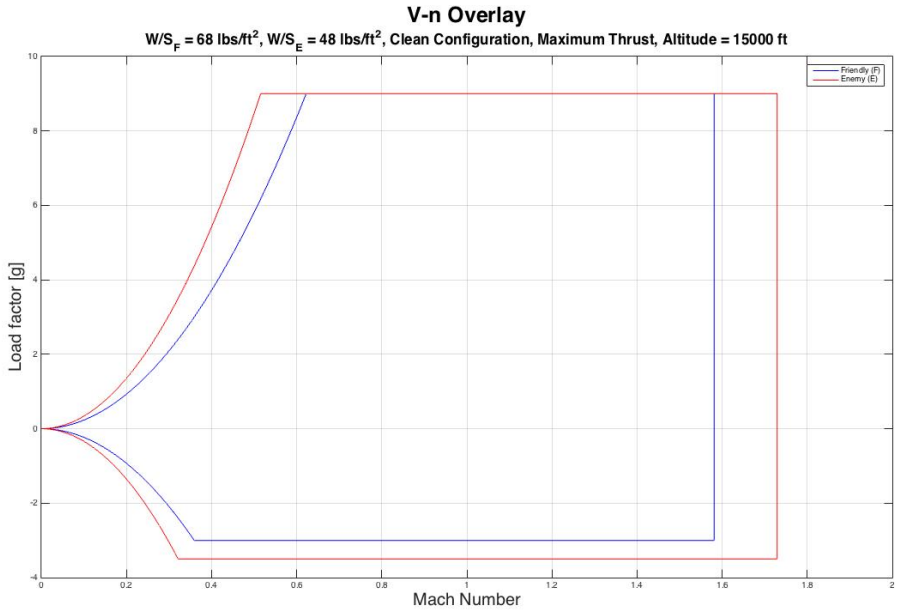

Figure 4.1 : V-n overlay of two fighters with different W/S

the adversary [4]. Figure 4.1 shows the V-n overlay of fighters with different wing loading (W/S). From the figure, it can be seen that fighter with lower wing loading has a significant advantage in instantaneous maneuverability. At a specific speed, the fighter with lower W/S can pull more (generate higher load factor) than its adversary. Furthermore, it has higher speed advantage than the fighter with higher W/S. It should be noted that fighter with higher speed advantage may not only dictate the combat terms but also leave the combat at will. However, the advantageous/disadvantageous regions expressed by the V-n overlay are solely instantaneous.

4.2 P_s Overlay

One of the most important applications of P_s diagram is the comparative P_s diagram of two combating fighters in air-to-air combat. The visualization of areas of advantage and disadvantage of two combating aircrafts can be done by comparing their P_s values [20]. It can be obtained by plotting the P_s diagrams of the fighters at the same chart (P_s overlay). P_s overlay helps combat planners in deciding in which region friendly fighter should attempt to engage enemy's fighter.

Generally, aircraft with higher P_s value has better maneuvering capability during combat. To gain offensive maneuvering advantage, first of all, a pilot is required to have an aircraft that has the ability to reach a higher positive P_s and then follow the

energy path that make the most of this advantage. In an air-to-air combat, a pilot who can attack and defend while maintaining a higher energy level than his/her adversary, owns maneuvering superiority. Even though a pilot starts the fight at lower energy level but if he/she can gain more energy than his enemy during the fight, he/she may enjoy maneuvering advantage [4]. Offensive maneuvering advantage belongs to a fighter, who can gain energy more rapidly or lose it less quickly. A pilot with a higher energy level has a better chance to enter or leave the fight as he/she wishes. On the other hand, a defender, which has the capability of losing energy faster than the attacker, may use this capacity to defend by pushing the attacker to overshoot and gain a momentary offensive maneuvering position [4, 24]. On that account, the amount of energy possessed and how well that energy is managed are the two important factors that determine the best maneuverability [4]. There is no obvious advantage if the difference in P_s between two fighters is less than 100 ft/s [29]. Area of advantage is defined as the area where an aircraft has P_s advantage higher than 100 ft/s over enemy aircraft.

The important elements shown by the P_s overlay are climbing, accelerating, low speed and high speed environment capabilities. P_s overlay can show which region is advantageous/disadvantageous/exclusive for one own's aircraft and an adversary aircraft. It can reveal which fighter has superior/inferior maneuvering capability at high and low altitudes and at high and low speeds. P_s overlay representation is valid for specific conditions of aircraft's weight, engine thrust, configuration and load factor. For example, as fighter starts to turn, its load factor changes and hence its corresponding P_s representation. Seeing that aerial combat requires a considerable amount of turning maneuvers, P_s diagram at higher load factors should also be plotted. This will help combat planners in obtaining a complete maneuvering presentation of fighter's tactical envelope. The variation in P_s of maneuvering fighters can also be shown by overlaying diagrams of different load factors for example, overlaying 2 g and 1 g diagrams [6]. Nevertheless, this representation can turn into a mess rapidly. In an air-to-surface combat, maneuvering capabilities and limitations with a large variety of stores or weaponries on board can also be determined using this diagram.

When $P_s = 0$ contour of an aircraft envelope that of the enemy, it means that friendly aircraft can fight enemy aircraft's maneuvers while losing less energy [8]. When

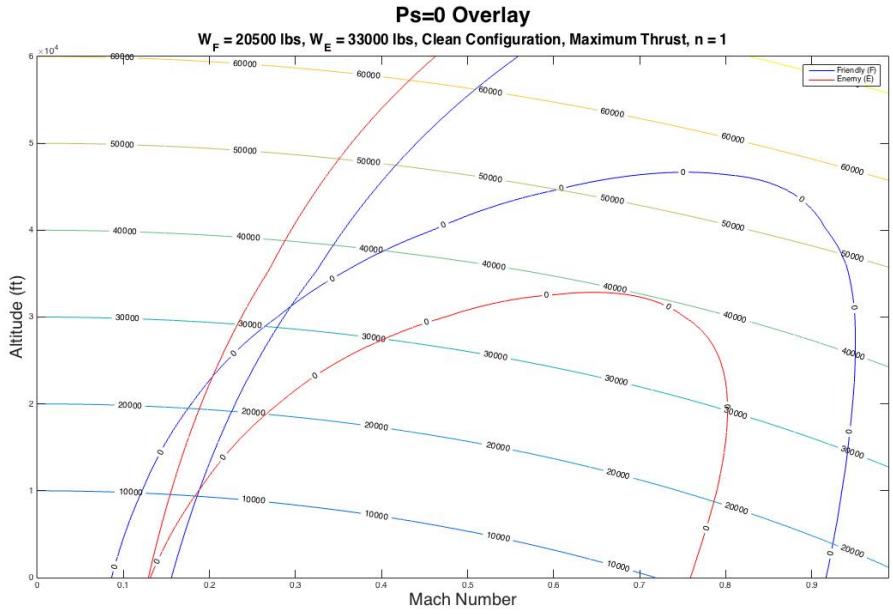

Figure 4.2 : P_s overlay of two fighters with different weights

friendly fighter can fly exclusively at a region of altitudes and velocities, which are outside of enemy fighter flight envelope, that region is defined as the exclusive area of the friendly fighter. Within that region, the P_s of the enemy fighter is negative and thus it will lose energy if it decides to fly with the altitude and airspeed combinations located inside.

Figure 4.2 is an example of $P_s = 0$ overlay of two aircrafts. The contours on the left side are the stall limits. From the figure, it can be seen that friendly aircraft has superior high altitude performance and high speed advantage, whereas enemy aircraft has small low speed advantage at lower altitudes. The diagram shows that friendly aircraft has higher rate of climb and acceleration capabilities than the enemy aircraft. Thus, if the two aircrafts challenge each other at the same altitude, friendly aircraft may climb away from the enemy aircraft to its maximum altitude, which is outside the operating envelope of the enemy aircraft, until it is advantageous to dive to attack. The capability of friendly aircraft to fly to higher altitudes means that it has higher potential energy that can be transformed to kinetic energy in a dive. In regions where the P_s contours overlap, both aircrafts have similar capability and thus only the combat skills of the pilots determine the combat outcome.

4.3 E-M Overlay

E-M diagram is a very useful tool in preparing aerial combat. In order to be able to determine how to use a fighter against a defined enemy, the E-M diagrams for both fighters can be overlaid. Similar with P_s overlay, E-M overlay shows advantageous/disadvantageous/exclusive regions of one own's fighter and an enemy fighter. As the E-M diagrams of the fighters overlap, it means that they have similar performance capabilities within that region and thus only the combat skills of the pilots participating in the fight determine the combat result. Therefore, pilot should make the most of the area of advantage and stay away from the area of disadvantage (the area of advantage of the enemy aircraft).

It is useful to incorporate P_s contours into E-M overlay. Nevertheless, as P_s contours are incorporated in the diagram, this representation can turn into a mess, similar to the P_s overlay technique described before. Therefore, instead of P_s contours, only the $P_s = 0$ contour that is drawn to mark the boundary of the region of gaining energy (positive P_s) and the region of losing energy (negative P_s). E-M diagram and hence E-M overlay is valid for specific operating conditions of power/thrust level, altitude, weight, and configuration. Therefore, to obtain a complete maneuvering presentation of the fighters, several diagrams depicting other operating conditions should be plotted.

Figure 4.3 is an example of E-M overlay between a friendly aircraft and an enemy aircraft. The $P_s = 0$ contour of the friendly aircraft envelopes that of the enemy aircraft, which means that it can maneuver with turn rate and speed combinations where enemy aircraft loses energy. Friendly aircraft has advantages both at high and low speed regions and can turn at higher rates than the enemy aircraft.

4.4 Comparison Results

In this study, fighter aircraft capability assessment is focused on E-M parameters such as P_s, load factor, turn rate and turn radius. When two fighters combat at the same airspeed, they possess different turn radius only if their turn rates are different. In this case, it may not be easy to see the benefit of having small turn radius. When the fighters are maneuvering at the same turn rate but at different airspeeds, the fighter with lower

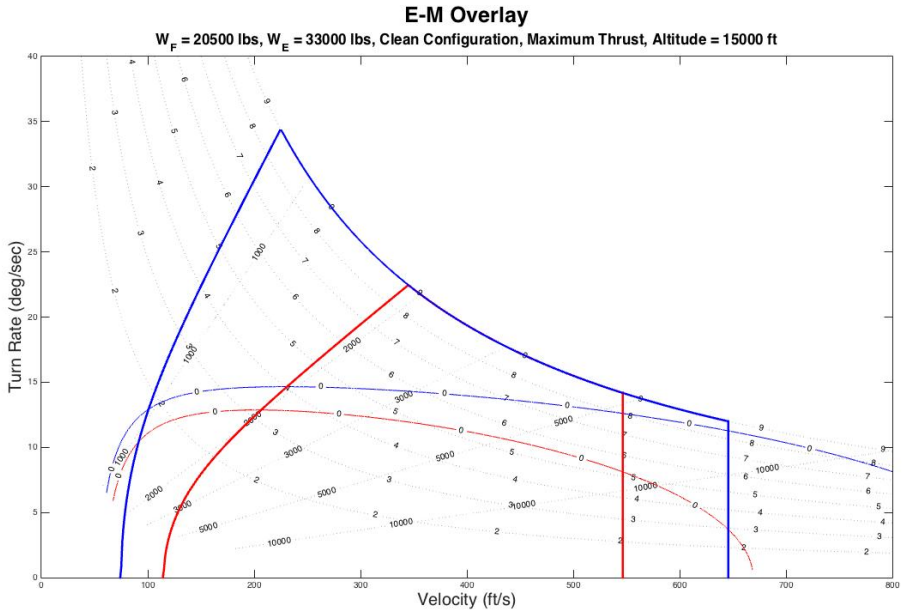

Figure 4.3 : E-M overlay of two fighters with different weights

speed will have smaller turn radius. As the turning maneuver continues, that fighter, which turns at lower speed, has the benefit of position advantage, which may allow it to shoot first.

It is not possible to maximize P_s and turn rate and minimize turn radius at the same time. At high energy state (high speed and high P_s), aircraft is capable at doing many maneuvers such as, climbing, turning and accelerating, yet turn rate and turn radius suffer. At low energy state (low speed and low P_s), turn radius decreases and turn rate increases whereas the aircraft is vulnerable to attacks as it does not have enough energy to do maneuvers. Therefore, careful examination to achieve a balance or compromise between those parameters should be done throughout combat planning.

Without access to complete military data, it is believed that the result of this study can only be considered as representative and that there is possibility of the existence of other results of such calculation. The aircraft data are from secondary source and some parameters are less certain due to the incompleteness of the data available. Nevertheless, the results appear to support the author's estimates.

5. DECISION PROCESS

This chapter will combine the results of simulation and discussions with a F-16 pilot from Indonesian Air Force (TNI AU), the air force branch of the Indonesian National Armed Forces. A decision process, which aims to give the best input strategy for fighter maneuvers, will be presented. The fundamental points during aerial combat are energy management and quick kill. Throughout the fight, pilot is usually required to perform several defensive and offensive maneuvers. Every maneuver ends either with energy being gained or expended. It is important to gain an energy advantage over the enemy and to avoid untimely loss of maneuvering energy. Higher energy level shows that fighter has greater capability to maneuver than its enemy. Thus, energy should not be expended either too fast or too large. However, sometimes depleting energy may be preferred in order to force the enemy to overshoot and to reach an advantageous position for a shooting opportunity.

Pilot usually monitors aircraft's energy through speed indicator in the cockpit and the relative position of the aircraft from the adversary. In general, bank angle and its rate are set according to the training procedures. Pilot generally uses ADI (Attitude Director Indicator) to know its magnitude. However, after several hundreds of flight hours, instead of using ADI, pilot uses his/her intuition to determine the magnitude of bank angle input. Usually, pilot specifies the maneuver inputs based on the lift vector position of the enemy aircraft. Therefore, during low yo-yo maneuver for example, the magnitude of bank angle input depends on the position of the adversary and the desired direction of the lift vector of the aircraft. For pitch angle and its rate, their magnitudes are set depending on the point in which the pilot is flying to relative to the adversary. This decision will determine for example the type of pursuit: lead, lag or pure.

In an effort to gain energy advantage, both opponents will trade altitude for airspeed or airspeed for altitude many times. Throughout combat, pilot must constantly evaluate his/her energy while at the same time assess the energy of the enemy. This information is necessary for a successful fight. In this study, the aerial maneuvers taken into account

are some basic fighter maneuvers such as aileron roll, immelmann, low yo-yo, and high yo-yo.

5.1 Aircraft Model

A 3-DOF aircraft performance model similar to that F-16 is used. Consider the aircraft system as $\dot{x} = f(x,u)$, where x is the state variable and u is the control input. The state variable x consists of $[x,y,h,V,\psi,m]$ while the control input u comprises $[\delta,\mu,\gamma]$. x,y,h,V,ψ,m are aircraft's position in the north direction, east direction, altitude, velocity, heading and mass, respectively. δ,μ,γ are throttle level, bank angle and path angle, respectively. Engine and aerodynamic data are provided in [30] and [31]. It is assumed that aircraft maneuvers over a short distance to the extent that the curvature and rotation of the earth are negligible. The equations of motion are given by:

$$\begin{aligned}
\dot{x} &= V\cos\psi\cos\gamma \\
\dot{y} &= V\sin\psi\cos\gamma \\
\dot{h} &= V\sin\gamma \\
\dot{V} &= \frac{1}{m}(T\cos\alpha - D) - g\sin\gamma \\
\dot{\psi} &= \frac{\sin\mu}{mV\cos\gamma}(T\sin\alpha + L) \\
\dot{m} &= -f
\end{aligned}$$

where α is angle of attack, g is gravitational constant, T is thrust, D is drag, L is lift and f is fuel flow rate. The aerodynamic forces D and L can be calculated as $D = 0.5\rho SV^2C_D$ and $L = 0.5\rho SV^2C_L$.

The aircraft is assumed to be at cruise condition as shown in Table 5.1. Detail explanation on each maneuver and aircraft model can be found in [32]. The table of input parameters used for simulation as given in [32] is reproduced in Table 5.2. Throughout combat, with the use of fuel and weaponries, the weight of the aircraft changes continuously. Nevertheless, during performance analysis, weight is taken as constant as the changes are small on the subject of maneuvering time frame.

Table 5.1 : Initial conditions of the aircraft

$x(m)$	$y(m)$	$h(m)$	$V(m/s)$	$\psi(rad)$
10,000	10,000	4,000	250	$\frac{\pi}{8}$

Table 5.2 : Input parameters for simulations

	$\mu_{desired}$	$\gamma_{desired}$	$\dot{\mu}_{desired}$	$\dot{\gamma}_{desired}$	$\dot{\mu}_{limit}$	$\dot{\gamma}_{limit}$	$\Delta h_{desired}$
Aileron Roll	-	-	40 °/s	-	-	-	-
Barrel Roll	-	30 °	40 °/s	-	-	90 °/s	-
Loop	-	-	-	40 °/s	-	-	-
Break Turn	80 °	-	-	-	90 °/s	-	-
Immelmann	-	-	-	40 °/s	90 °/s	-	-
Split S	-	-	-	40 °/s	90 °/s	-	-
Vertical Spiral	80 °	30 °	-	-	90 °/s	90 °/s	500 m
Spiral Dive	80 °	30 °	-	-	90 °/s	90 °/s	500 m
Low Yo-Yo	65 °	30 °	-	-	90 °/s	90 °/s	500 m
High Yo-Yo	65 °	30 °	-	-	90 °/s	90 °/s	500 m

5.2 Selected Metrics

The amount of energy expended depending on the variation of maneuver input parameter will be evaluated. However, determining the best input strategy cannot be done by only analyzing the energy depleted during the maneuver. The pilot from TNI AU emphasized several times that energy management and quick kill are fundamental points during combat. Furthermore, other parameters such as load factor, velocity, turn rate, and P_s variation throughout maneuver should also be taken into account. It is important that during maneuver, aircraft does not exceed its maximum and minimum load factor, stall speed, maximum speed, and maximum turn rate limitations. Moreover, for future maneuver sequences, turning capability (turn rate and turn radius) at the end of the maneuver should be evaluated.

In order to assess the maneuver time, energy expended, and constraints variation of the aircraft during maneuver, several metrics will be used. These metrics are selected from the discussion performed in Chapter 2. They are maneuver time, energy-agility

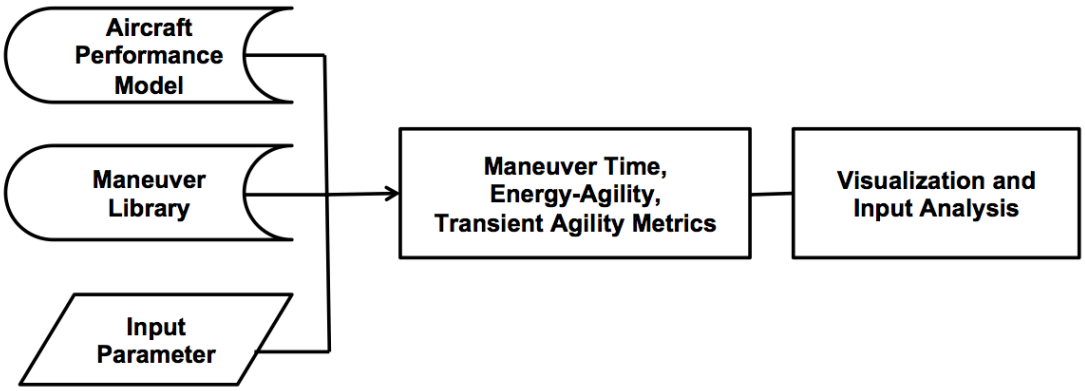

Figure 5.1 : Steps involved in the decision process

plot, and transient agility parameters plot. Outline of the steps involved in the decision process is given in Figure 5.1.

5.2.1 Maneuver time

The time to perform a task was first introduced by Skow in [26]. A timeline for a mission profile sequence was given in order to find out which component of an aircraft weapon system causes large time delays in an engagement. Delays due to pilot, pilot-vehicle interface, flight control systems, airframe and weapon are included to find the overall time from target detection to target destruction. In [16], the time to perform a task is classified into operational agility metric. It quantifies all the delays due to pilot, avionics, airframe and weapon related to a mission task. Nevertheless, in this study, only aircraft or airframe agility will be taken into account. Therefore, maneuver time metric parameter merely measures the time required to perform a maneuver.

5.2.2 Energy-agility

The calculation of the energy expended is based on the Energy Agility concept, which was first introduced in [25]. This metric modeled the time to kill, the time to kill and recover and the energy compromised. Its plot is called the energy-agility plot and it gives the specific energy (E_s) variation of the aircraft throughout the maneuver. The area between the initial specific energy level and the time-energy curve quantifies the amount of energy lost during the maneuver. In this study, the energy-agility metric is used to measure only the energy compromised to complete a specific maneuver. No time to kill and time to kill and recover variables are given.

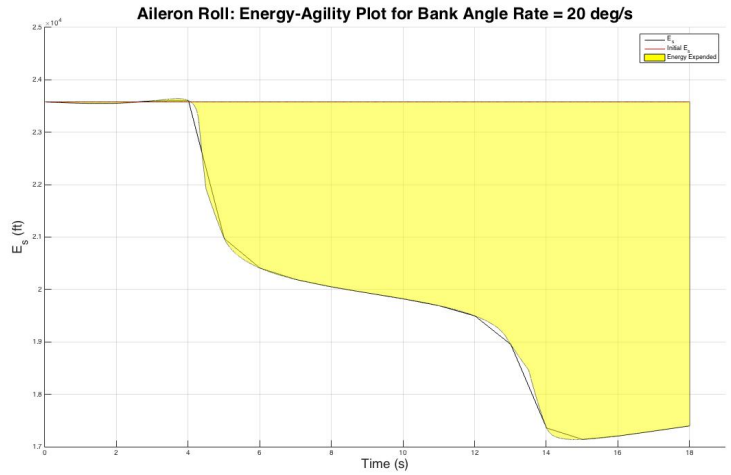

Figure 5.2 : Energy-agility of aileron roll for $\dot{\mu} = 20$ °/s

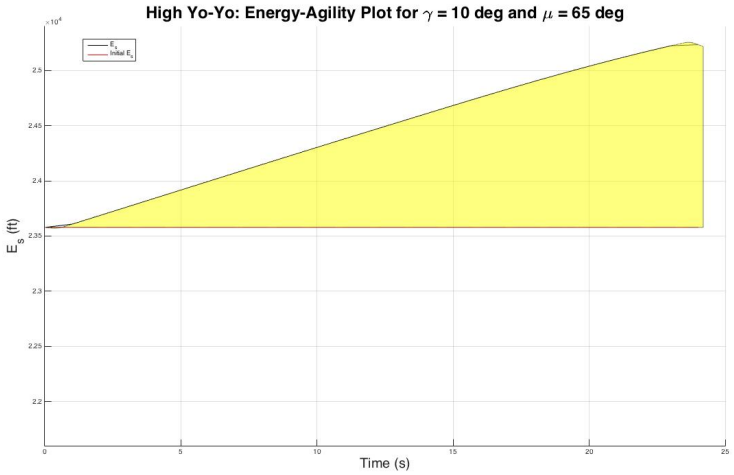

Figure 5.3 : Energy-agility of high yo-yo for $\gamma = 10$ °& $\mu = 65$ °

In general, the time-energy curve lies below the initial specific energy (E_{s_i}) level line. This is because energy is typically consumed during maneuver. The total energy at the end is usually less than the total energy at the beginning of the maneuver. Nevertheless, there are several maneuvers with several input magnitudes, which have their time-energy curve lies above the E_{s_i} line. In this case, energy is not expended but energy is gained and the total energy at the end is higher than the initial total energy. Thus, in the case where the area between the E_{s_i} line and the time-energy curve is shaded, it means that energy is expended. In the case where the area between the time-energy curve and the E_{s_i} line is shaded, it shows that energy is gained. Examples are shown in Figure 5.2 and Figure 5.3.

Figure 5.2 shows that aircraft loses energy by performing aileron roll for $\dot{\mu} = 20$ °/s. This loss of energy was caused by the fact that throughout the maneuver, aircraft

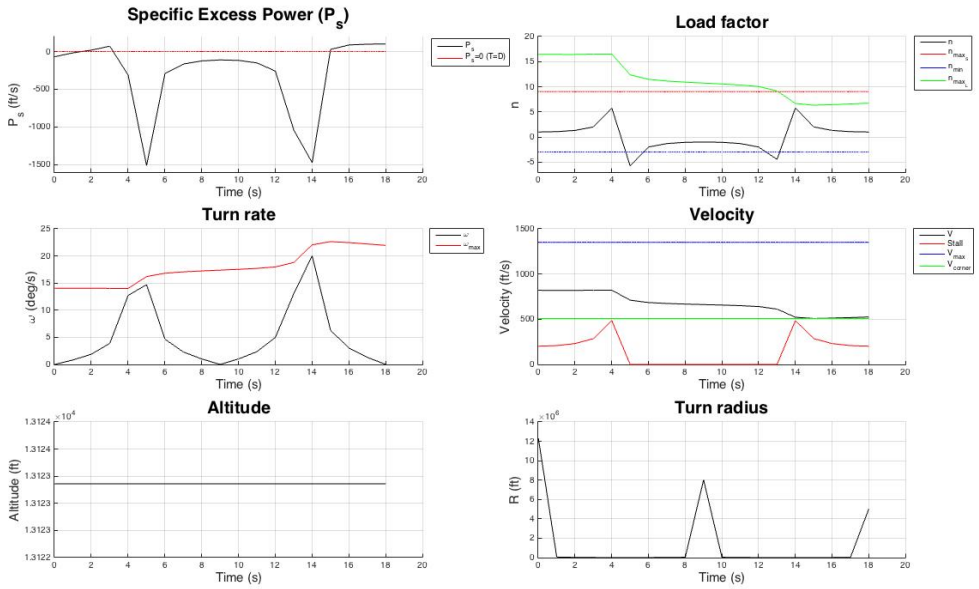

Figure 5.4 : Transient agility plots of aileron roll for $\dot{\mu} = 20$ °/s

speed keeps decreasing as can be seen in the V plot of Figure 5.4. Calculation using MATLAB shows that the amount of energy expended is 6,108,769.5 ft.s. Figure 5.3 reveals that energy is gained after completing high yo-yo maneuver for $\gamma = 10$ °and $\mu = 65$ °. Energy is gained because throttle level is kept at a constant value in order to prevent airspeed from decreasing. Calculation shows that the sum of energy gained is 2,103,733.4 ft.s.

For simplicity, since there are cases where throughout maneuver, aircraft might either gain or lose energy depending on the magnitude of the input parameter, only energy expended parameter is shown in the plots and tables. Positive value signifies the amount of energy depleted while negative value denotes the sum of energy gained.

5.2.3 Transient agility

The transient agility metric contains parameters such as P_s, ω, n, V, R, and h. In [16], the energy-maneuverability parameters, P_s, ω, and n are classified into transient agility metrics. Other parameters are also given, but only P_s, ω, and n satisfy all the attribute codes. This fact supports the author's assumption that the traditional performance measures of merit still actually can be used to assess the agility of modern fighter aircrafts. The demonstration of the metric information is attained through time history plots. Example is shown in Figure 5.4.

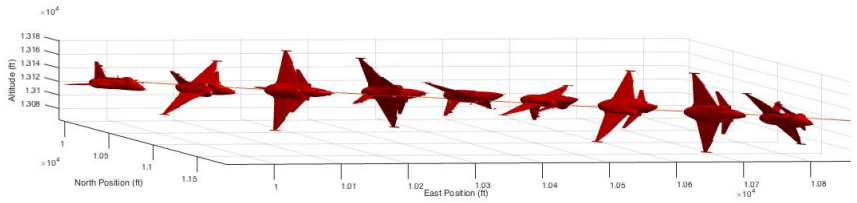

Figure 5.5 : Aileron roll trajectory for $\dot{\mu} = 40$ °/s

5.3 Simulation

5.3.1 Aileron roll

Aileron roll is a maneuver where aircraft turns 360°along longitudinal axis while flying straight and level. Example trajectory of the aircraft performing aileron roll maneuver with $\dot{\mu}$=40 °/s bank rate input is shown in Figure 5.5.

5.3.1.1 Maneuver time

Plot of maneuver time to variation in $\dot{\mu}$ is given in Figure 5.6. It can be seen that as $\dot{\mu}$ increases, maneuver time decreases.

5.3.1.2 Energy-agility

The energy-agility plots of the aircraft performing aileron roll maneuver with different bank rate inputs ($\dot{\mu}$=20 °/s, 40 °/s, 80 °/s, 90 °/s) are given in Figure 5.7a to Figure 5.7d. The area shaded in yellow indicates the energy expended. As it can be seen from the figures, as bank angle rate increases, the shaded area decreases. This shows that $\dot{\mu}_{limit} = 90°/s$ gives the least energy lost. The results are tabulated in Table 5.3. Plot of energy expended to variation in $\dot{\mu}$ is given in Figure 5.8. It can be seen that as $\dot{\mu}$ increases, energy depleted decreases.

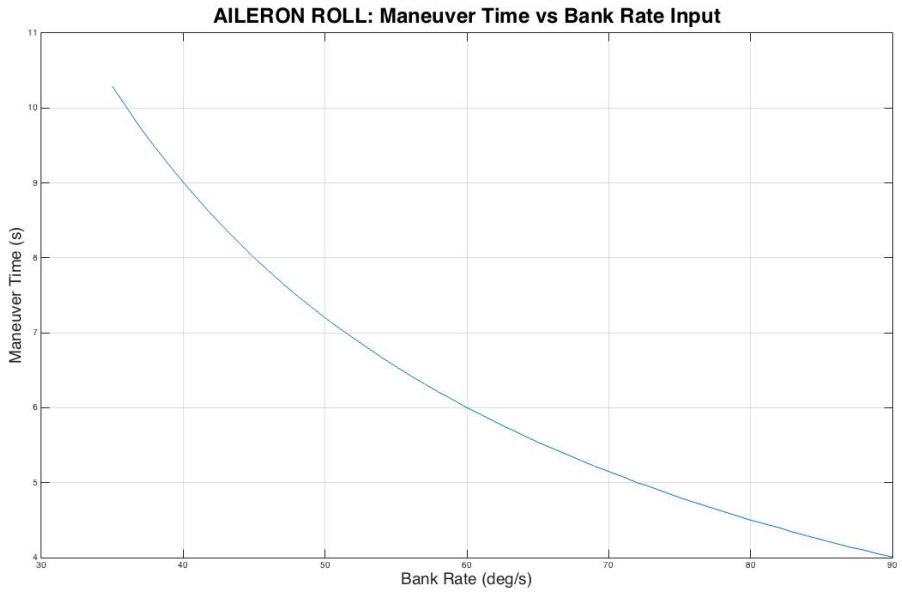

Figure 5.6 : Aileron roll: maneuver time vs bank rate

Table 5.3 : Aileron roll

$\dot{\mu}$	**20 °/s**	**40 °/s**	**80 °/s**	**90 °/s**
E_{s_i} **(ft)**	23,579.4	23,579.4	23,579.4	23,579.4
Maneuver time (s)	18.01	9.01	4.5	4.01
Reference energy (ft.s)	42,442,999.2	21,221,499.6	10,587,170.4	9,431,777.6
Energy expended (ft.s)	6,108,769.5	1,756,278.3	477,345.8	386,870.5

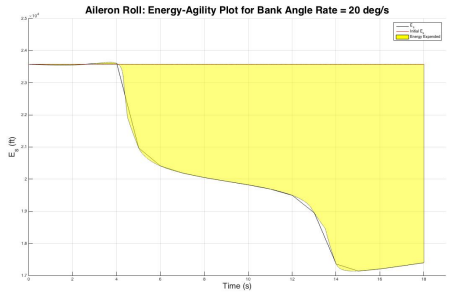

(a) $\dot{\mu} = 20$ °/s

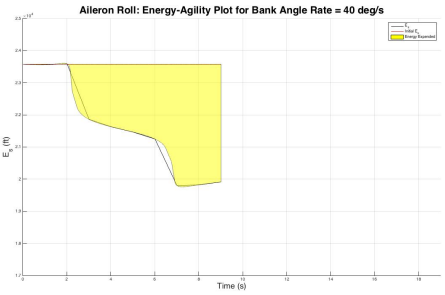

(b) $\dot{\mu} = 40$ °/s

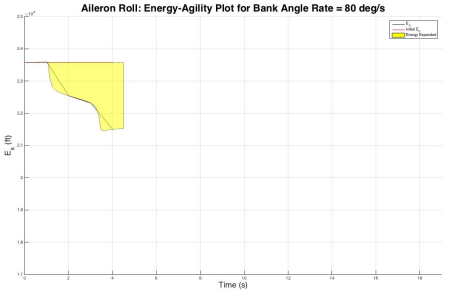

(c) $\dot{\mu} = 80$ °/s

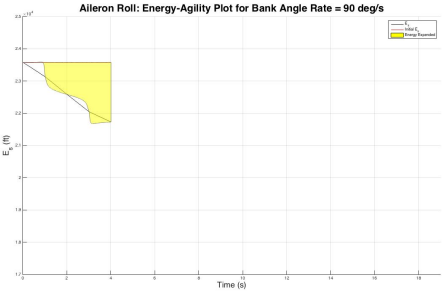

(d) $\dot{\mu} = 90$ °/s

Figure 5.7 : Energy-agility of aileron roll

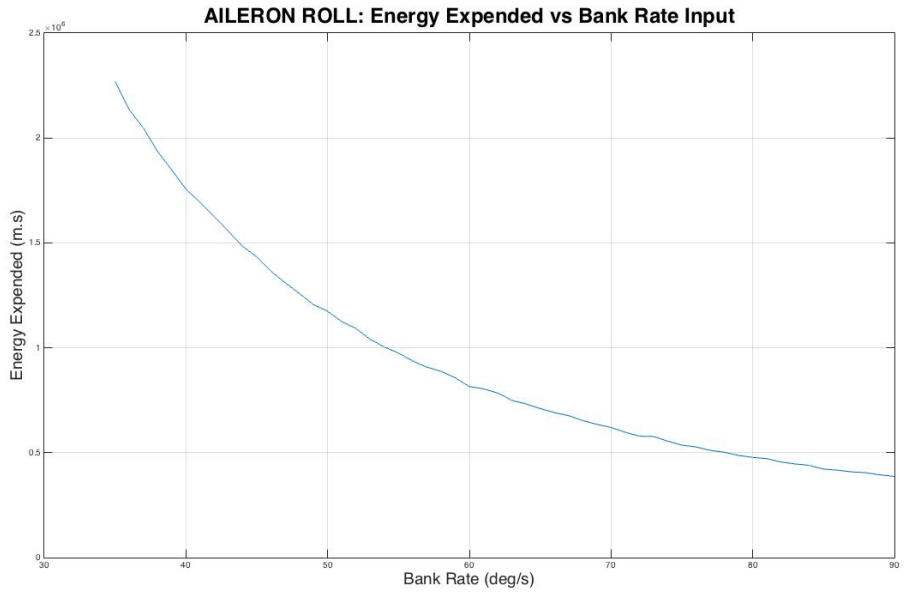

Figure 5.8 : Aileron roll: energy expended vs bank rate

5.3.1.3 Transient agility

From Table 5.3, by considering only the energy-agility and maneuver time metrics for $\dot{\mu}$=20 °/s, 40 °/s, 80 °/s, 90 °/s, either $\dot{\mu} = 80$ °/s or $\dot{\mu} = 90$ °/s can be seen as the best input strategy. The transient agility metric parameters variation for both inputs are given in Figure 5.9a to Figure 5.9b. From Figure 5.9b, it can be observed that $\dot{\mu} = 90$ °/s is not the best input strategy, since it causes the aircraft to exceed its maximum load factor and maximum turn rate limits. This input also causes the aircraft to undergo a very large negative P_s variation. Furthermore, at the end of the maneuver, aircraft will be at a point where it has no more turning capability.

On the contrary, from Figure 5.9a, it can be seen that $\dot{\mu} = 80$ °/s does not cause the aircraft to violate its velocity, load factor and turn rate limitations. At the end of the maneuver, aircraft has positive P_s value and adequate turning capability for the next sequence of maneuver. Thus, in this case, $\dot{\mu} = 80$ °/s is the best input strategy.

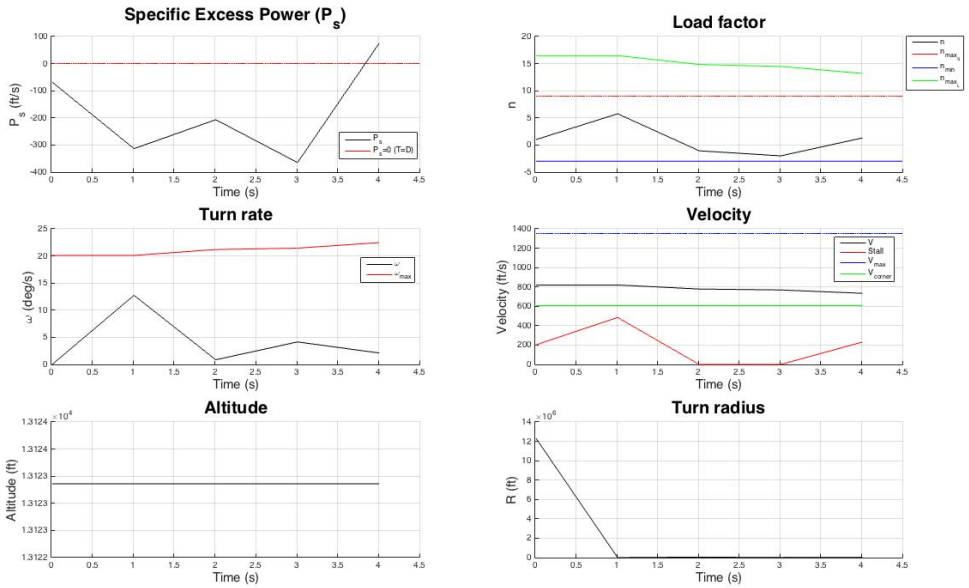

(a) $\dot{\mu} = 80$ °/s

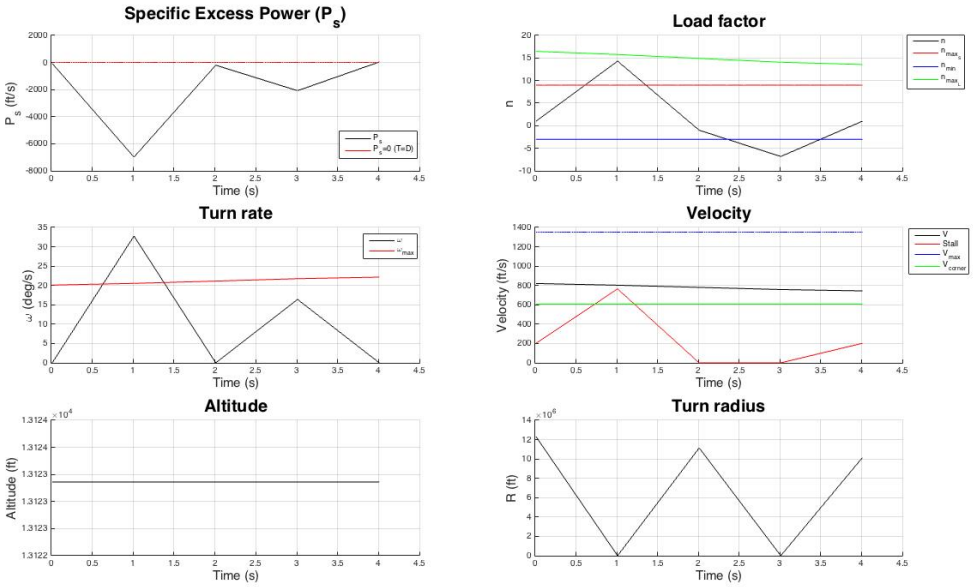

(b) $\dot{\mu} = 90$ °/s

Figure 5.9 : Transient agility plots of aileron roll

5.3.2 Immelmann

Immelmann is used to reverse heading and gain altitude. A half of a loop is executed by pitching the nose up and climbing and then inverting to terminate. Aircraft will be flying at a higher altitude in a different direction. Example trajectory of the aircraft performing immelmann maneuver with $\dot{\gamma}$=40 °/s is shown in Figure 5.10.

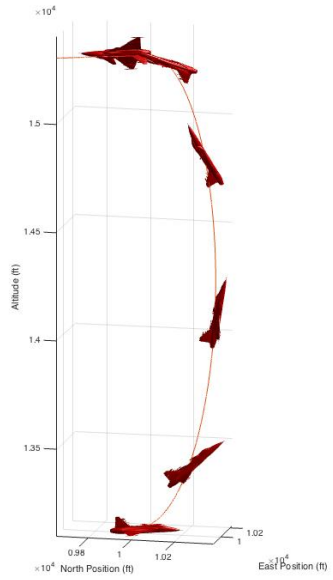

Figure 5.10 : Immelmann trajectory for $\dot{\gamma} = 40$ °/s

5.3.2.1 Maneuver time

Plot of maneuver time versus $\dot{\gamma}$ is given in Figure 5.11. It can be seen that as $\dot{\gamma}$ increases, maneuver time decreases.

5.3.2.2 Energy-agility

The energy-agility plots of the aircraft performing immelmann with different $\dot{\gamma}$ ($\dot{\gamma}$=20 °/s, 40 °/s, 80 °/s, 90 °/s) are given in Figure 5.12a to Figure 5.12d. The area shaded in yellow indicates the energy expended. From the figures, it can be seen that as $\dot{\gamma}$ increases, the shaded area decreases. The results are tabulated in Table 5.4. Plot of energy expended versus $\dot{\gamma}$ is given in Figure 5.13. It also shows that as $\dot{\gamma}$ increases, energy depleted decreases.

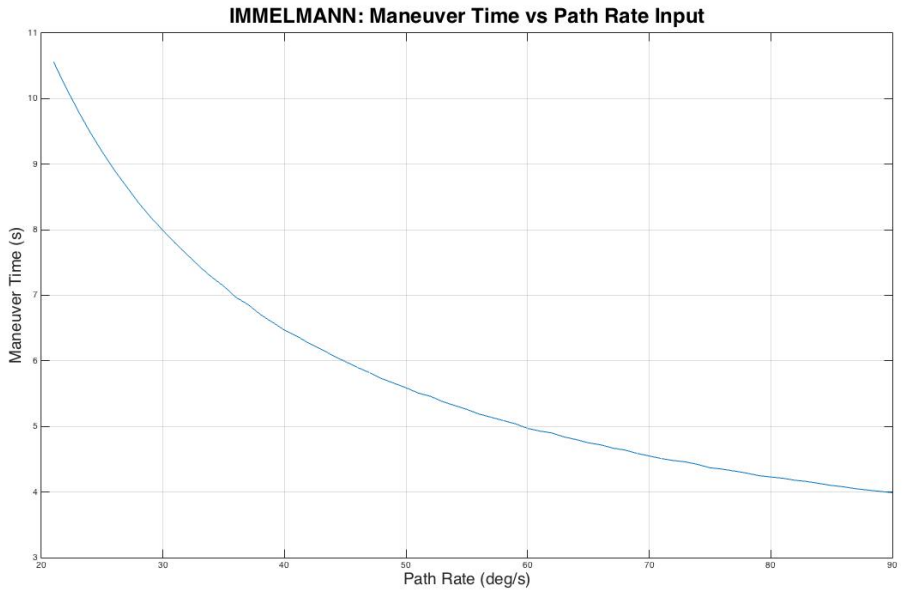

Figure 5.11 : Immelmann: maneuver time vs path rate

Table 5.4 : Immelmann

$\dot{\gamma}$	**20 °/s**	**40 °/s**	**80 °/s**	**90 °/s**
E_{s_i} **(ft)**	23,579.4	23,579.4	23,579.4	23,579.4
Maneuver time (s)	10.97	6.47	4.23	3.99
Reference energy (ft.s)	25,843,070.6	15,232,320.8	9,950,525.3	9,384,618.7
Energy expended (ft.s)	395,309.8	251,931.2	174,440.2	166,720.9

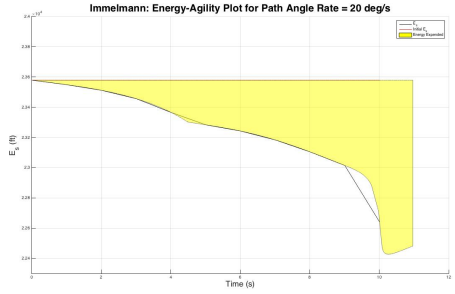

(a) $\dot{\gamma} = 20$ °/s

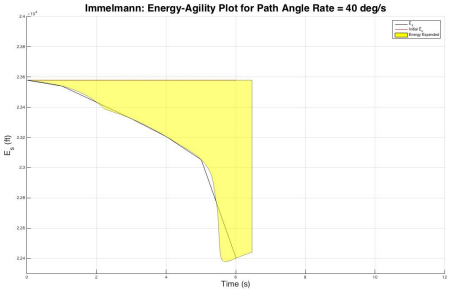

(b) $\dot{\gamma} = 40$ °/s

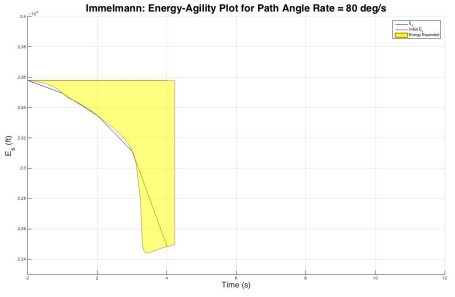

(c) $\dot{\gamma} = 80$ °/s

(d) $\dot{\gamma} = 90$ °/s

Figure 5.12 : Energy-agility of immelmann

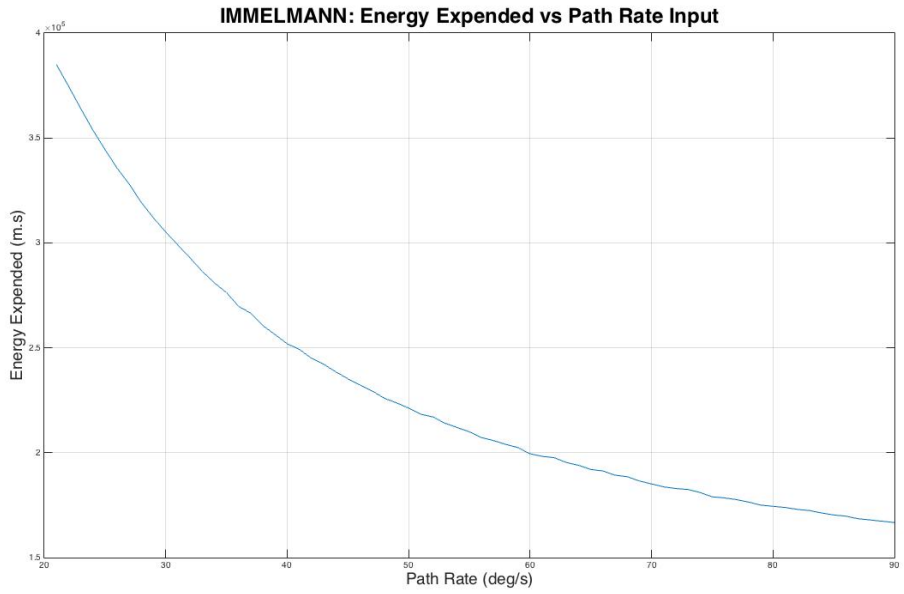

Figure 5.13 : Immelmann: energy expended vs path rate

5.3.2.3 Transient agility

From Table 5.4, by considering only the energy-agility and maneuver time metrics for $\dot{\gamma}$=20 °/s, 40 °/s, 80 °/s, 90 °/s, $\dot{\gamma} = 90$ °/s can be seen as the best input strategy, which gives the least maneuver time and energy expended. Transient agility metric plots for $\dot{\gamma} = 40$ °/s, $\dot{\gamma} = 80$ °/s and $\dot{\gamma} = 90$ °/s are given in Figure 5.14a to Figure 5.14c. From the figures, it can be seen that $\dot{\gamma} = 90$ °/s causes the aircraft to undergo a very large negative P_s variation. It also causes the aircraft to exceed its maximum load factor and maximum turn rate limits, which leave the aircraft with no turning capability at the end of the maneuver.

On the contrary, $\dot{\gamma} = 40$ °/s and $\dot{\gamma} = 80$ °/s do not cause the aircraft to violate its load factor, velocity, and turn rate limitations. Even though $\dot{\gamma} = 80$ °/s yields less energy expended than $\dot{\gamma} = 40$ °/s, at the end of the maneuver, $\dot{\gamma} = 40$ °/s leaves the aircraft with higher turn rate and lower turn radius turning capability than $\dot{\gamma} = 80$ °/s. Moreover, $\dot{\gamma} = 40$ °/s gives less variation in negative P_s and put the aircraft at a higher P_s value compared to $\dot{\gamma} = 80$ °/s. In combat counting in more than two participants, it is important to keep energy for future maneuvers. The aircraft, which is at a higher positive P_s value than its adversary, owns maneuvering superiority. Therefore, in this case, $\dot{\gamma} = 40$ °/s is the best input strategy.

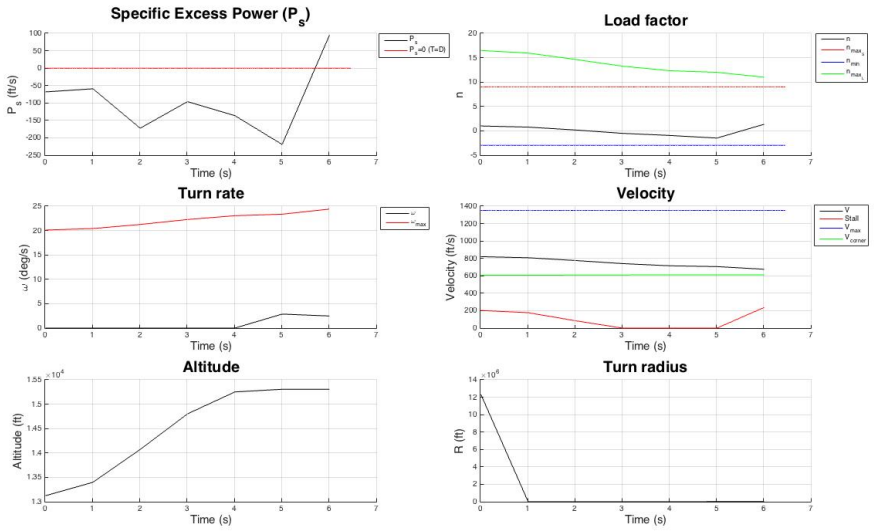

(a) $\dot{\gamma} = 40$ °/s

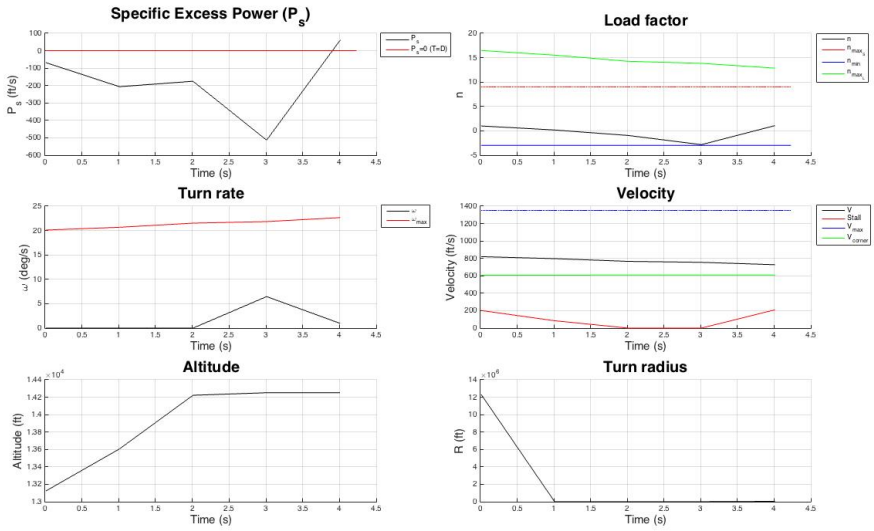

(b) $\dot{\gamma} = 80$ °/s

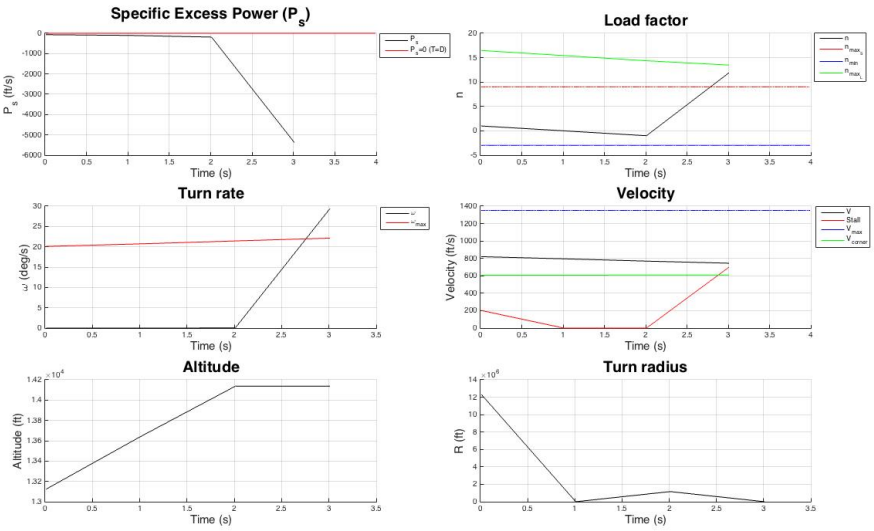

(c) $\dot{\gamma} = 90$ °/s

Figure 5.14 : Transient agility plots of immelmann

5.3.3 Low yo-yo

Low yo-yo is a lead pursuit maneuver, which decreases range at the cost of increasing angle off tail. Sometimes, this maneuver is performed when pilot is stuck in lag pursuit and has low closure rate due to airspeed superiority of the adversary. Thus, in order to gain velocity, pilot dives inside the target's turn and then pitching up onto its tail. It is not suggested to perform this maneuver at low altitude. Example trajectory of the aircraft performing low yo-yo maneuver for $\gamma = 30\ ^\circ$, $\mu = 65\ ^\circ$is shown in Figure 5.15.

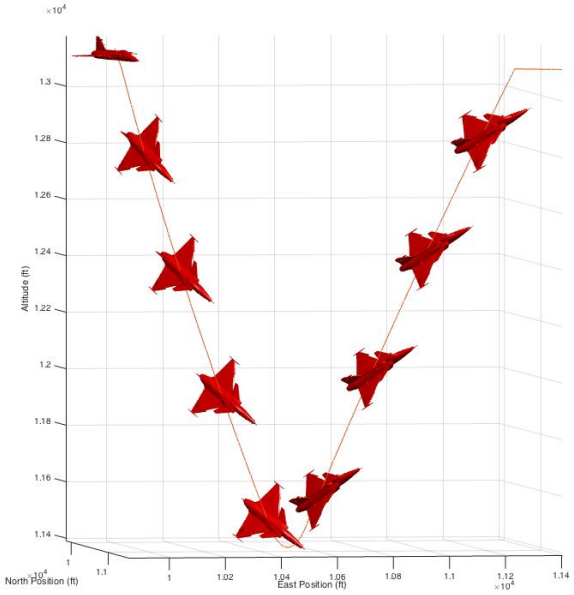

Figure 5.15 : Low yo-yo trajectory for $\gamma = 30\ ^\circ$, $\mu = 65\ ^\circ$

5.3.3.1 Maneuver time

Plot of maneuver time to bank angle variation for $\gamma = 30\ ^\circ$is given in Figure 5.16. As bank angle increases, maneuver time increases slightly up to $\mu = 80\ ^\circ$. Plot of maneuver time to path angle variation for $\mu = 65\ ^\circ$is given in Figure 5.17. At low path angle, maneuver time is large. There is a steep decrease in maneuver time between $\gamma = 1\ ^\circ$and $\gamma = 10\ ^\circ$. Above $\gamma = 10\ ^\circ$, the decrement occurs slightly. Surface plot of maneuver time to bank and path angle inputs variations is given in Figure 5.18.

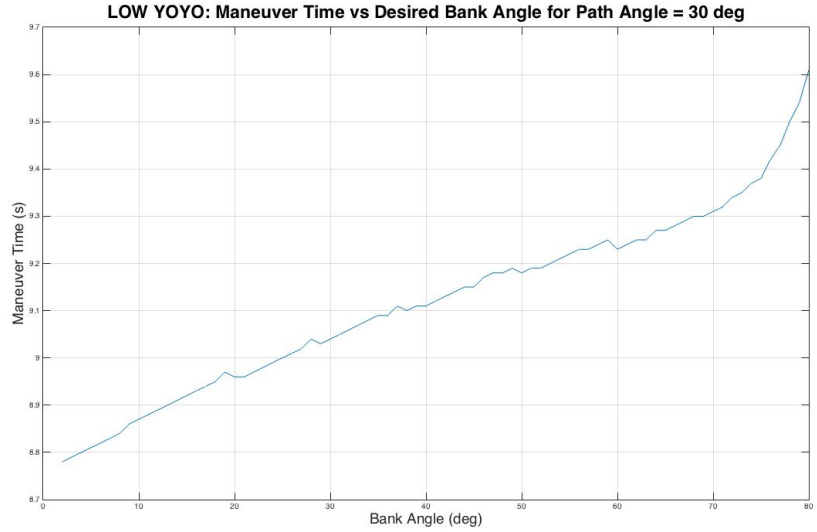

Figure 5.16 : Low yo-yo: maneuver time vs desired μ for $\gamma = 30\ ^\circ$

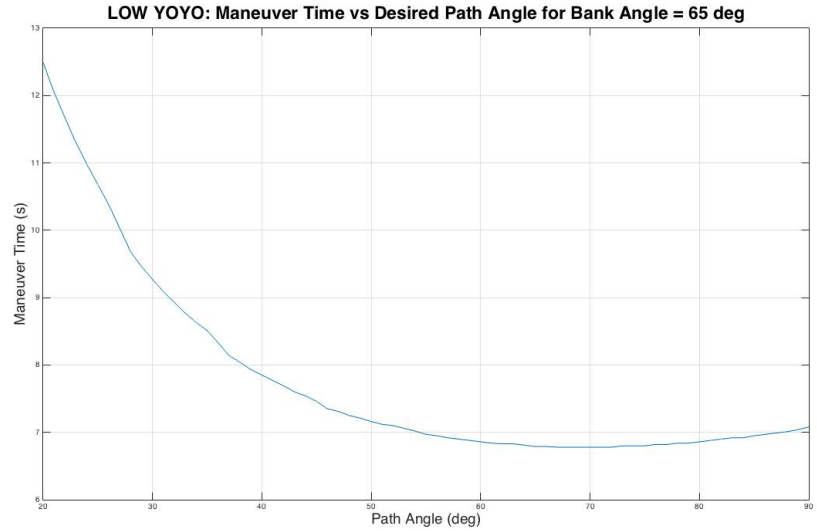

Figure 5.17 : Low yo-yo: maneuver time vs desired γ for $\mu = 65\ ^\circ$

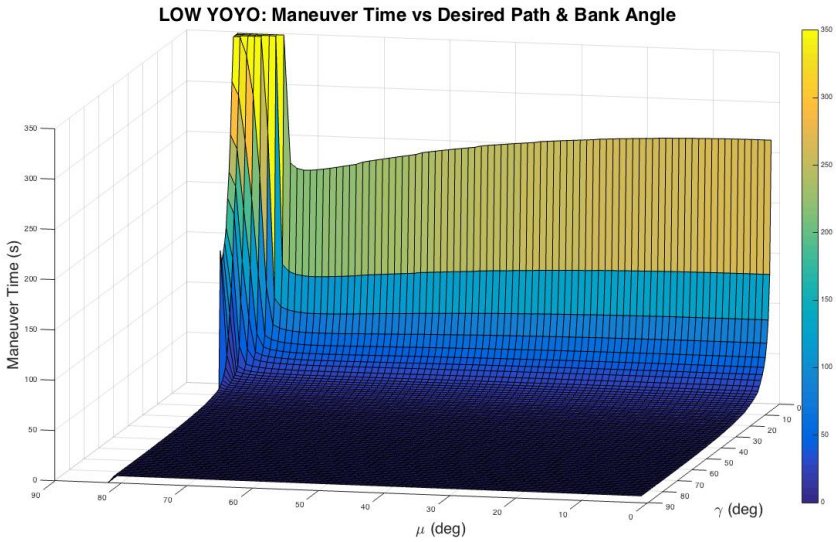

Figure 5.18 : Low yo-yo: maneuver time vs desired μ and γ

Table 5.5 : Low yo-yo

γ, μ	$\gamma = 10$ °, $\mu = 65$ °	$\gamma = 30$ °, $\mu = 65$ °	$\gamma = 30$ °, $\mu = 80$ °
E_{s_i} **(ft)**	23,579.4	23,579.4	23,579.4
Maneuver time (s)	22.78	9.27	9.61
Reference energy (ft.s)	53,690,394	21,834,565.1	22,636,266.2
Energy expended (ft.s)	-1,383,175.2	-171,367.9	386,891.4

5.3.3.2 Energy-agility

Energy-agility plots of the aircraft performing low yo-yo with three different path and bank angle inputs combinations ($\gamma = 10$ °& $\mu = 65$, $\gamma = 30$ °& $\mu = 65$ °, $\gamma = 30$ °& $\mu = 80$ °) are shown in Figure 5.19a to Figure 5.19c. The area shaded in yellow indicates the energy expended or gained. The results are tabulated in Table 5.5.

Plot of energy expended to bank angle variation for $\gamma = 30$ °is given in Figure 5.20. As bank angle increases up to $\mu = 55$ °, energy expended decreases. Between $\mu = 55$ °and $\mu = 78$ °, energy is gained while above $\mu = 78$ °, there is a steep increase in energy expended. Plot of energy expended to path angle variation for $\mu = 65$ °is given in Figure 5.21. At low path angle energy gained is large. There is a steep decrease in energy gained between $\gamma = 1$ °and $\gamma = 10$ °. Above $\gamma = 10$ °, the decrement occurs slightly. Approximately above $\gamma = 51$ °, instead of gained, energy is expended. Surface plot of energy expended/gained to bank and path angle input variations is given in Figure 5.22.

5.3.3.3 Transient agility

Transient agility metric plots of low yo-yo with three different input combinations are given in Figure 5.23a to Figure 5.23c. For $\gamma = 10$ °, $\mu = 65$ °, aircraft suffers from long maneuver time but gains large amount of energy. That input combination also allows the aircraft to have positive P_s value and good turning capability at the end of the maneuver. For $\gamma = 30$ °, $\mu = 65$ °, even though aircraft gains energy, at the end of the maneuver, it has negative P_s and poor turning capability. For $\gamma = 30$ °, $\mu = 80$ °, despite the fact that at the end aircraft reaches positive P_s value, it experiences large negative P_s variation and loses energy throughout the maneuver. Thus, from these three examples, $\gamma = 10$ °and $\mu = 65$ °is the best input strategy.

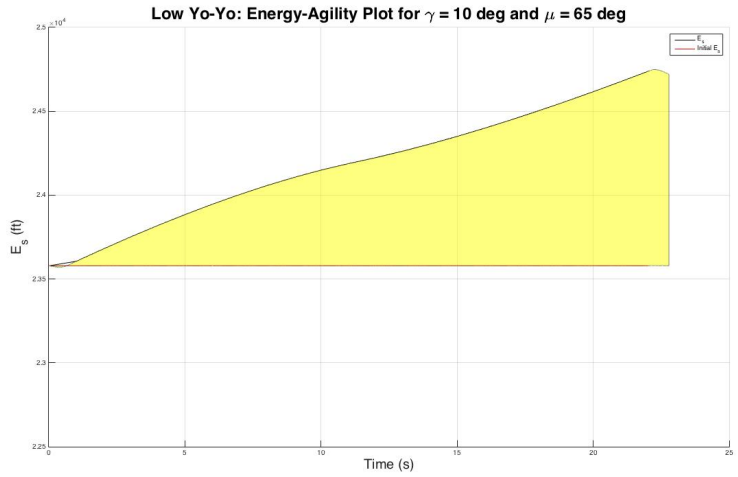

(a) $\gamma = 10\ ^\circ$, $\mu = 65\ ^\circ$

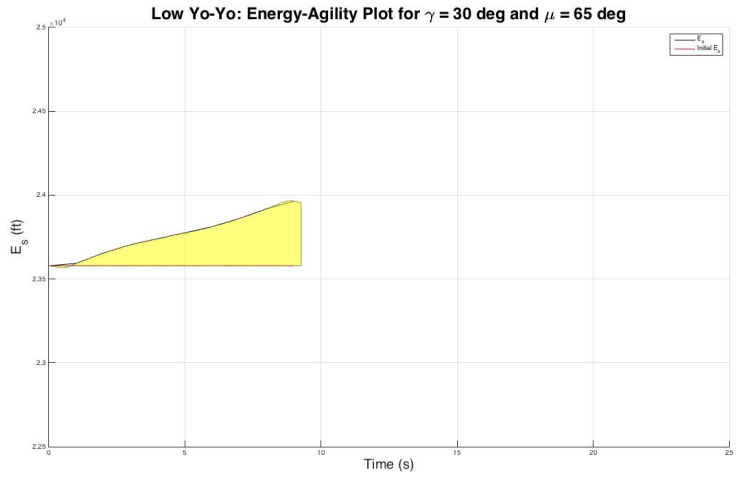

(b) $\gamma = 30\ ^\circ$, $\mu = 65\ ^\circ$

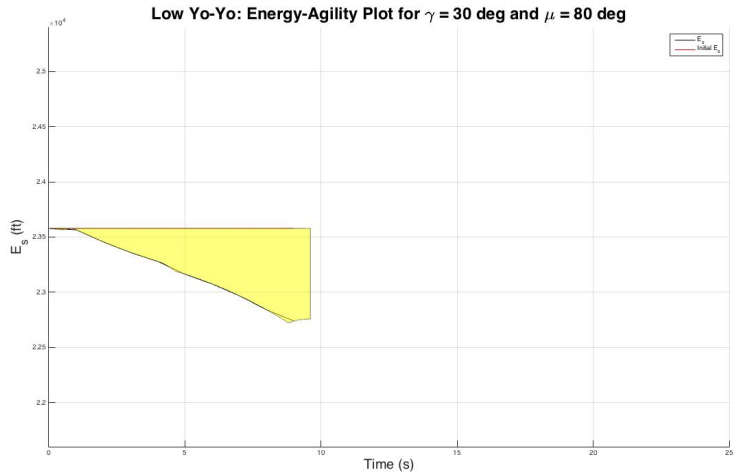

(c) $\gamma = 30\ ^\circ$, $\mu = 80\ ^\circ$

Figure 5.19 : Energy-agility of low yo-yo

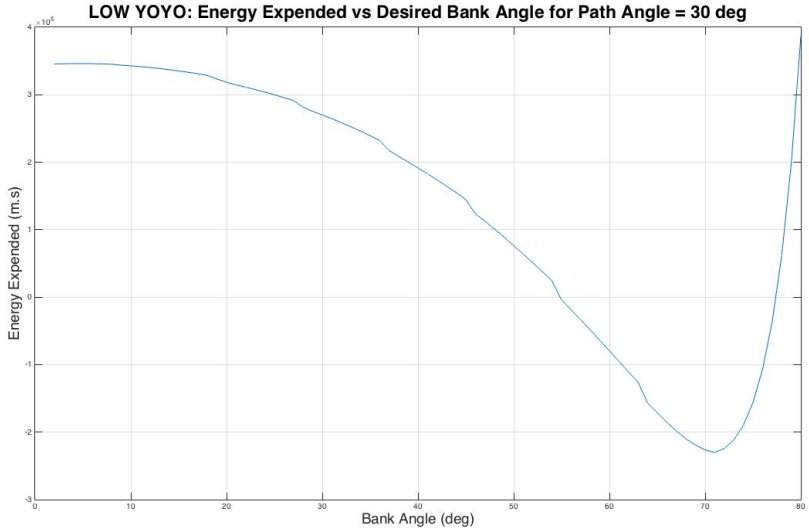

Figure 5.20 : Low yo-yo: energy expended vs desired μ for $\gamma = 30$ °

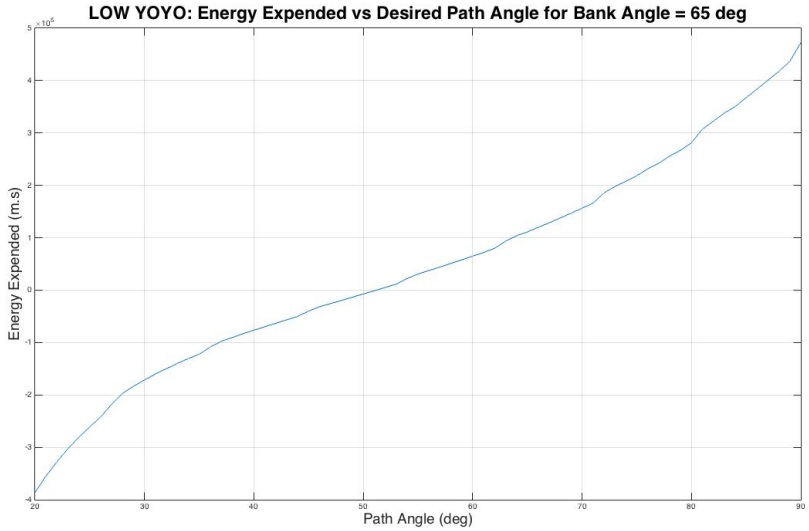

Figure 5.21 : Low yo-yo: energy expended vs desired γ for $\mu = 65$ °

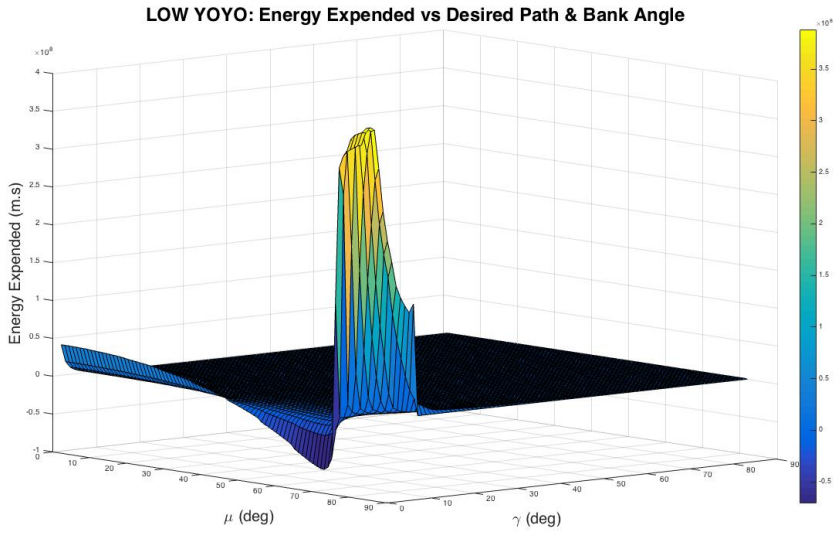

Figure 5.22 : Low yo-yo: energy expended vs desired μ and γ

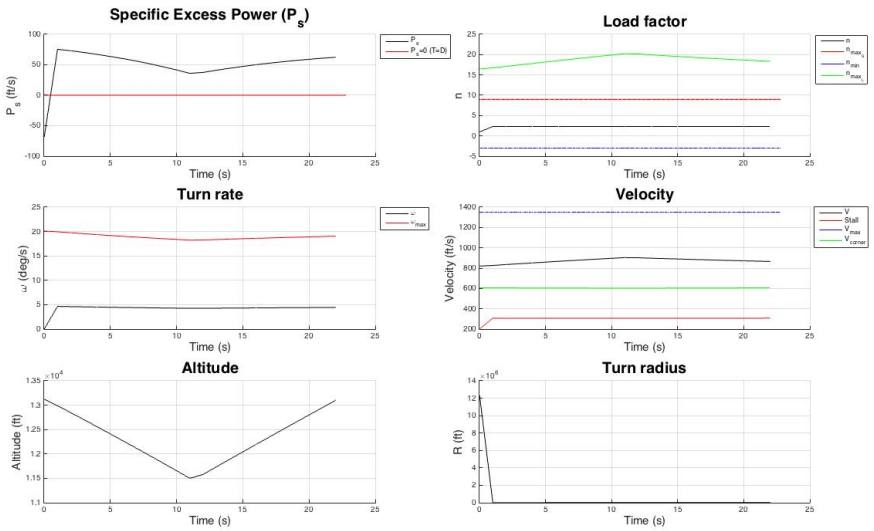

(a) $\gamma = 10\ ^\circ$, $\mu = 65\ ^\circ$

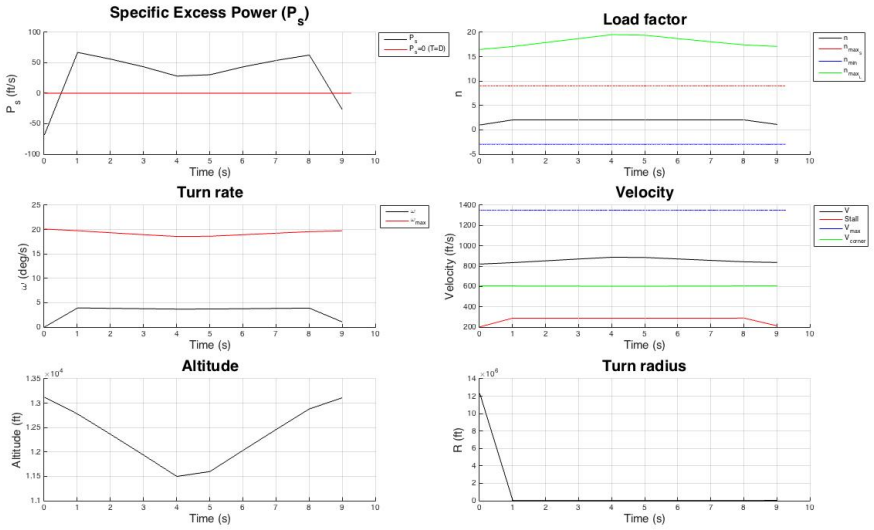

(b) $\gamma = 30\ ^\circ$, $\mu = 65\ ^\circ$

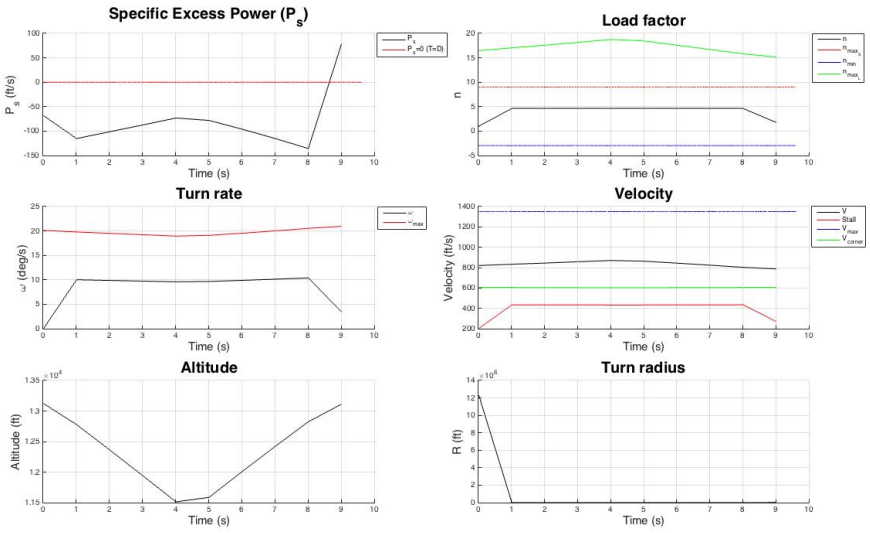

(c) $\gamma = 30\ ^\circ$, $\mu = 80\ ^\circ$

Figure 5.23 : Transient agility plots of low yo-yo

5.3.4 High yo-yo

High yo-yo, the inverse of low yo-yo, is an offensive lag pursuit maneuver. It reduces the angle off tail at the cost of increasing the distance between the aircraft and the adversary. The maneuver is started by a slight roll followed by pulling the nose up. To terminate, roll back toward the inside of the adversary's turn at a smaller angle off tail. Sometimes, this maneuver is performed in order to avoid overshooting the target due to the high closure rate of the aircraft. To prevent the enemy from accelerating out of range, it is important not to lose too much speed during the climbing portion of the maneuver. Example trajectory of the aircraft performing high yo-yo maneuver for $\gamma = 30$ °and $\mu = 65$ °is shown in Figure 5.24.

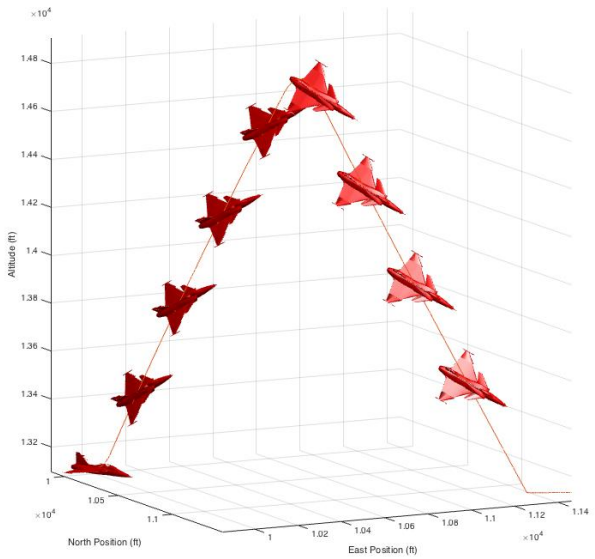

Figure 5.24 : High yo-yo trajectory for $\gamma = 30$ °, $\mu = 65$ °

5.3.4.1 Maneuver time

Plot of maneuver time to bank angle variation for $\gamma = 30$ °is given in Figure 5.25. As bank angle increases, maneuver time increases slightly up to $\mu = 80$ °. Above $\mu = 80$ °, there is a steep increase in maneuver time. Plot of maneuver time to path angle variation for $\mu = 65$ °is given in Figure 5.26. At low path angle, maneuver time is large. There is a steep decrease in maneuver time between $\gamma = 1$ °and $\gamma = 10$ °. Above $\gamma = 10$ °, the decrement occurs slightly. Surface plot of maneuver time to bank and path angle inputs variations is given in Figure 5.27.

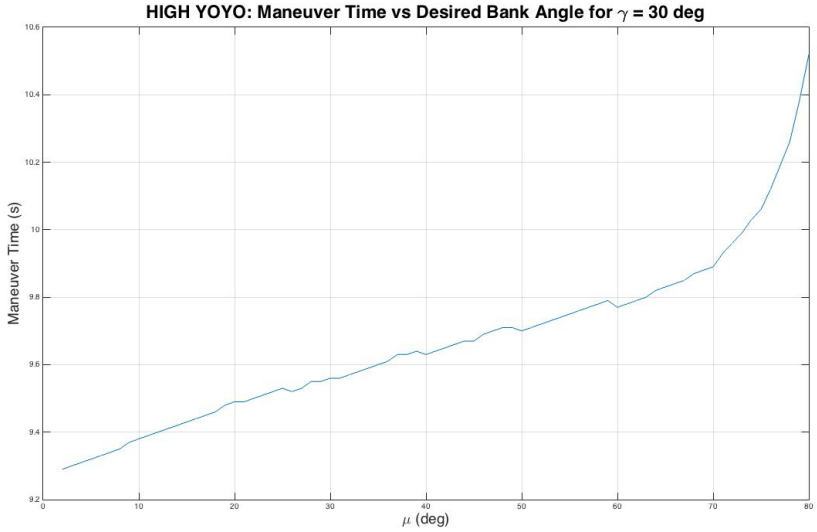

Figure 5.25 : High yo-yo: maneuver time vs desired μ for $\gamma = 30$ °

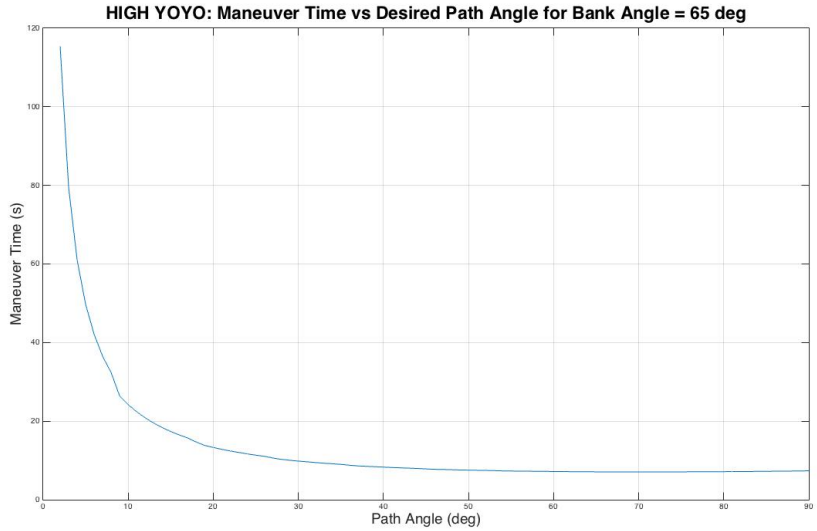

Figure 5.26 : High yo-yo: maneuver time vs desired γ for $\mu = 65$ °

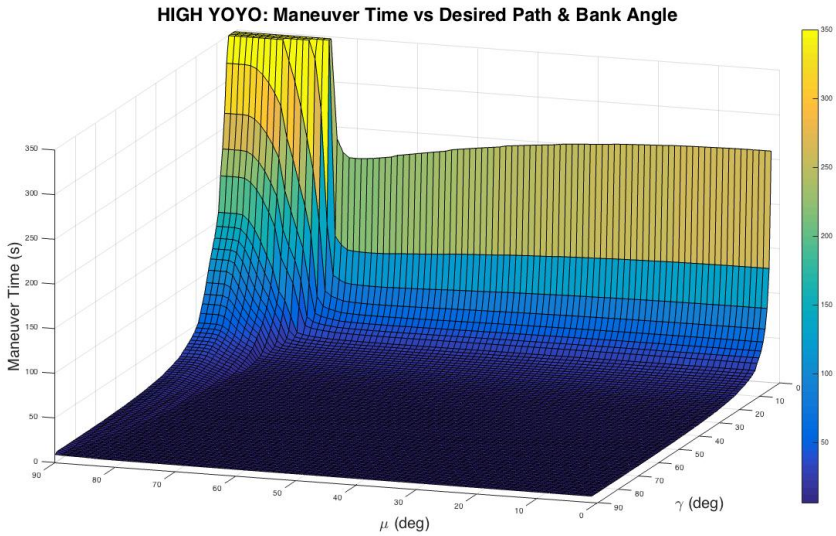

Figure 5.27 : High yo-yo: maneuver time vs desired μ and γ

Table 5.6 : High yo-yo

γ, μ	$\gamma = 10$ °, $\mu = 65$ °	$\gamma = 30$ °, $\mu = 65$ °	$\gamma = 30$ °, $\mu = 80$ °
E_{s_i} **(ft)**	23,579.4	23,579.4	23,579.4
Maneuver time (s)	24.19	9.83	10.52
Reference energy (ft.s)	57,015,095.6	23,155,014	24,781,995.6
Energy expended (ft.s)	-2,103,733.4	-330,238.5	933,264.2

5.3.4.2 Energy agility

Energy-agility plots of the aircraft performing high yo-yo with three different path and bank angle inputs combinations ($\gamma = 10$ °& $\mu = 65$, $\gamma = 30$ °& $\mu = 65$ °, $\gamma = 30$ °& $\mu = 80$ °) are shown in Figure 5.28a to Figure 5.28c. The area shaded in yellow indicates the energy expended or gained. The results are tabulated in Table 5.6.

Plot of energy expended to bank angle variation for $\gamma = 30$ °is given in Figure 5.29. As bank angle increases up to $\mu = 20$ °, energy expended decreases. Between $\mu = 20$ °and $\mu = 75$ °, energy is gained while above $\mu = 75$ °, there is a steep increase in energy expended. Plot of energy expended to path angle variation for $\mu = 65$ °is given in Figure 5.30. At low path angle, energy gained is large. There is a steep decrease in energy gained between $\gamma = 1$ °and $\gamma = 10$ °. Above $\gamma = 10$ °, the decrement occurs slightly. Approximately above $\gamma = 71$ °, instead of gained, energy is expended. Surface plot of energy expended/gained to bank and path angle inputs variations is given in Figure 5.31.

5.3.4.3 Transient agility

Transient agility metric plots of high yo-yo with three different input combinations are given in Figure 5.32a to Figure 5.32c. For $\gamma = 10$ °, $\mu = 65$ °, even though aircraft gains large amount of energy, it suffers from long maneuver time. At the end of the maneuver, aircraft has negative P_s and poor turning capability. For $\gamma = 30$ °, $\mu = 65$ °, at the end of the maneuver, aircraft gains energy, has positive P_s and good turning capability. For $\gamma = 30$ °, $\mu = 80$ °, even though at the end aircraft reaches positive P_s, but throughout the maneuver, it undergoes large negative P_s variation and loses a large amount of energy. Hence, from these three examples, $\gamma = 30$ °and $\mu = 65$ °is the best input strategy.

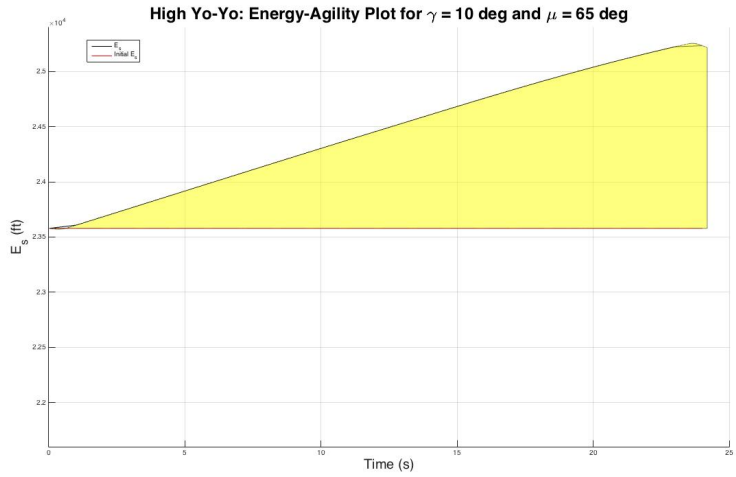

(a) $\gamma = 10\ ^\circ$, $\mu = 65\ ^\circ$

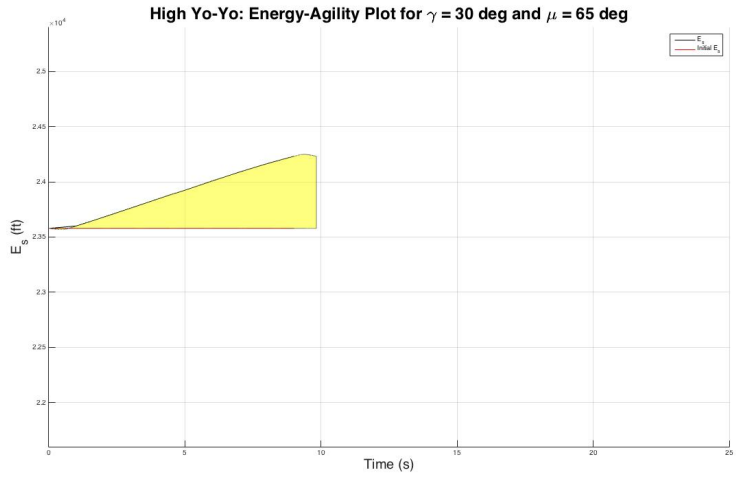

(b) $\gamma = 30\ ^\circ$, $\mu = 65\ ^\circ$

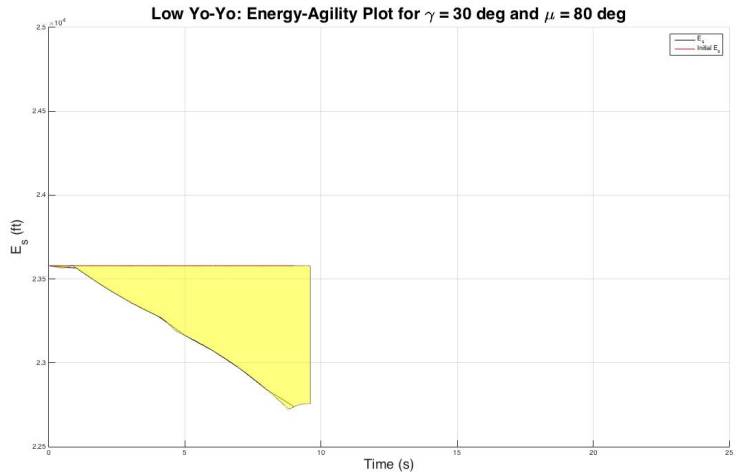

(c) $\gamma = 30\ ^\circ$, $\mu = 80\ ^\circ$

Figure 5.28 : Energy-agility of high yo-yo

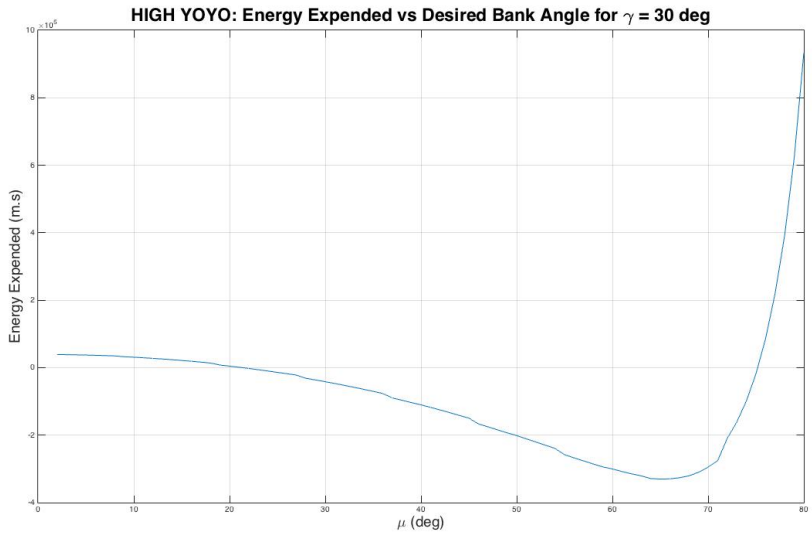

Figure 5.29 : High yo-yo: energy expended vs desired μ for $\gamma = 30$ °

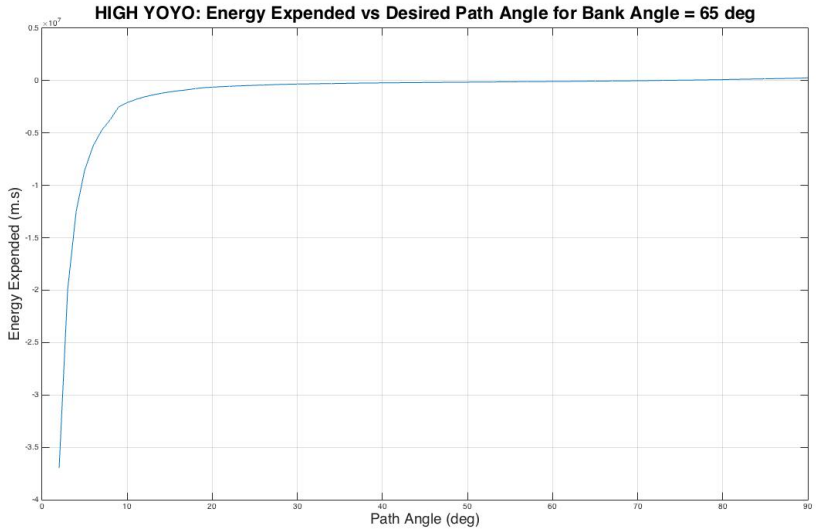

Figure 5.30 : High yo-yo: energy expended vs desired γ for $\mu = 65$ °

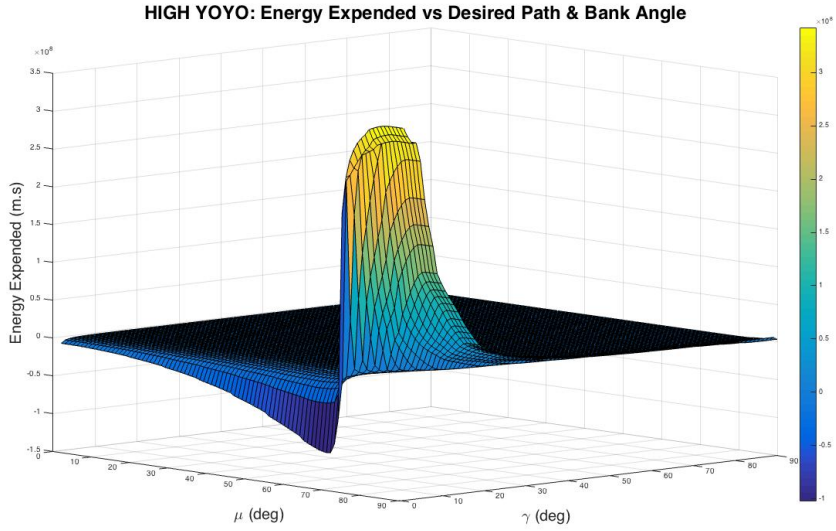

Figure 5.31 : High yo-yo: energy expended vs desired μ and γ

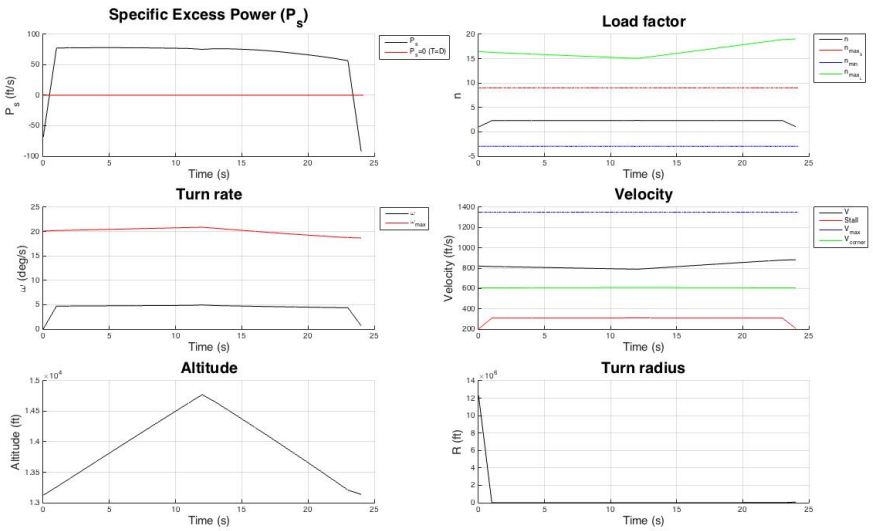

(a) $\gamma = 10\ ^\circ$, $\mu = 65\ ^\circ$

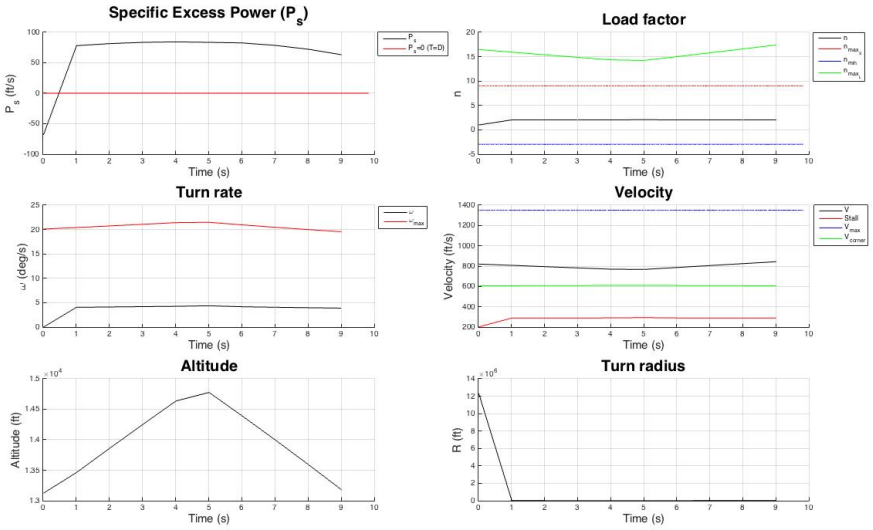

(b) $\gamma = 30\ ^\circ$, $\mu = 65\ ^\circ$

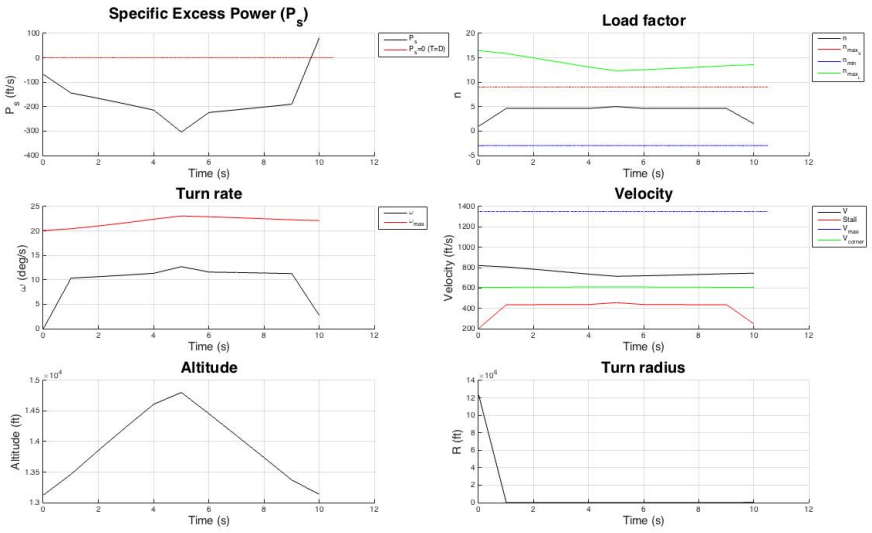

(c) $\gamma = 30\ ^\circ$, $\mu = 80\ ^\circ$

Figure 5.32 : Transient agility plots of high yo-yo

6. CONCLUSIONS AND FURTHER WORK

6.1 Conclusions

The primary rules for a successful aerial combat are quick kill, energy management, and assessment of transient characteristics. During combat, pilot must continuously evaluate his/her energy while at the same time assess the energy of the enemy. It is important to keep energy for future maneuvers especially in aerial fight counting in more than two participants. Thus, energy should not be expended either too fast or too large. The assessment of aircraft transient characteristics allows us to give a final remark in determining the best input strategy for fighter maneuvers.

In the near future, the significance of fighter maneuverability to win an aerial combat may be debatable. The important characteristic may shift for example from fighters capability to missiles capability. Missiles and radar technology developed more frequently than fighters technology. To win the fight, fighters may only need to carry sufficient amount of missiles and possess excellent radar and self-defense capabilities. Other than speed and E-M parameters superiority, weaponries, range capability, radar systems (detection of the enemy), the ability to evade detection by the enemy, the availability of airborne refuelling, and pilot capability are other key factors that determine the effectiveness and the outcome of a combat. Therefore, careful examination to achieve a balance or compromise between those parameters should be done throughout combat planning.

6.2 Further Work

Fighter assessment using point-mass aircraft model that we have done until now allows us to estimate fighter combat capabilities at determined flight conditions. In a highly dynamic situation, they provide analysis only of a particular point in the flight envelope. In order to have a complete analysis of dynamic maneuvering capabilities, instead of point-mass aircraft model, a full six degrees of freedom model is required.

The envelopes generated using energy analysis only represent the maneuvering capability of the aircraft but not of the pilot-aircraft system. Even though the aircraft is able to maneuver at the region of high g-loading, due to extended exposure to high g-loads, the capabilities of the pilot may decrease. Therefore, other than unmanned computer simulations, a thorough testing with man-in-the-loop simulations should be performed to obtain more realistic and adaptable combat tactics.

REFERENCES

[1] **Cox, W.B.** & **Downing, D.R.** (1992). Evaluation of functional agility metrics for fighter class aircraft, *AIAA-92-4487-CP*.

[2] **Bitten, R.** (1990). Qualitative and quantitative comparison of government and industry agility metrics, *Journal Aircraft*, *27*(3), 276 – 282.

[3] **Kutschera, A.** & **Render, P.M.** (October 1999). Design tools for performance assessment of fighter aircraft incorporating new technologies, *NATO Research and Technology Agency, Advanced Vehicle Technology Symposium*.

[4] **Boyd, J.R.**, **Christie, T.P.** & **Gibson, J.E.** (1966). Energy-maneuverability, *Technical Report*, Air Providing Ground Center, Eglin AFB, FL.

[5] **Shaw, R.L.** (1985). Fighter combat tactics and maneuvering, Naval Institute Press Annapolis, MD, USA.

[6] **Gallagher, G.L.**, **Higgins, L.B.**, **Khinoo, L.A.** & **Pierce, P.W.** (1992). U.S. Navy test pilot school flight test manual, Fixed Wing Performance *USNTPS-FTM-NO.108*.

[7] **Greene, T.E.** & **Huntzicker, J.H.** (1968). Simulation techniques for analyzing air combat systems, *The RAND Corporation*, Santa Monica, California.

[8] **Render, P.M.** (2010). Maneuver of fixed-wing combat aircraft. IN: Blockley, R., Shyy, W. (eds.). Encyclopedia of Aerospace Engineering, John Wiley and Sons, Inc.

[9] **Liefer, R.K.** (1990). Fighter agility metrics, *Paper No NASA-CR-187289*.

[10] **Pohlman, M.** & **Kam, C.** (2007). Energy based aerodynamic modeling: increasing fidelity of fixed-wing constructive entities, *Proceedings of the 2007 Spring Simulation Multiconference at Norfolk VA*, USAF, 327 – 336.

[11] **Tamrat, B.F.** (1988). Fighter aircraft agility assessment concepts and their implication on future agile fighter design, *AIAA-88-4400-CP, AIAA Aircraft Design, Systems and Operations Meeting*, Atlanta, Georgia.

[12] **McAtee, T.P.** (1988). Agility in demand, *Aerospace America*, 36 – 38.

[13] **Kutschera, A.** & **Render, P.M.** (August 2002). Advanced combat aircraft performance assessment, *The Aeronautical Journal*, 443 – 451.

[14] **Liefer, R.K.**, **Valasek, J.**, **Eggold, D.P.** & **Downing, D.R.** (1992). Fighter agility metrics, research and test, *Journal of Aircraft*, *29*(3), 452 – 457.

[15] **Valasek, J.** & **Downing, D.R.** (1993). An investigation of fighter aircraft agility-final, *Technical Report, KU-FRL-831-7*, Kansas University Flight Research Laboratory.

[16] **North Atlantic Treaty Organization. Advisory Group for Aerospace Research and Development**. (1994). Operational agility: La maniabilite operationnelle. Neuilly sur Seine, France: North Atlantic Treaty Organization, Advisory Group for Aerospace Research and Development.

[17] **Butts, S.L.** & **Lawless, A.R.** (1990). Flight testing for aircraft agility, *AIAA-90-1308-CP*.

[18] **Pruitt, V.R.**, **Moroney, W.F.** & **Lau, C.** (1980). Energy maneuverability display for the air combat maneuvering range/tactical training system (ACMR/TACTS), *Special Report 80-4*, Naval Aerospace Medical Research Laboratory.

[19] **Venable, J.** (2016). Operational assessment of the F-35A argues for full program procurement and concurrent development process, *Backgrounder*, *No. 3140*, *August 4, 2016*, The Heritage Foundation.

[20] **Liefer, R.K.** (1990). Fighter aircraft agility, *Ph.D. thesis*, University of Kansas.

[21] **Spearman, M.L.** (1984). Some fighter aircraft trends, *AIAA-84-2503-CP, AIAA Aircraft Design, Systems and Operations Meeting*, San Diego, CA.

[22] **Rutowski, E.S.** (1954). Energy approach to the general aircraft performance problem, *Journal of The Aeronautical Science*.

[23] **Nicolai, L.M.** & **Carichner, G.E.** (2010). Fundamentals of aircraft and airship design. Reston, VA: American Institute of Aeronautics and Astronautics.

[24] **Anon.** (1986). U.S. Air Force test pilot school performance phase textbook, *USAF-TPS-CUR-86-01*.

[25] **Dorn, M.D.** (1989). Aircraft agility: the science and the opportunities, *AIAA-89-2015-CP, AIAA/AHS/ASEE Aircraft Design, Systems and Operations Conderence, Seattle, WA*.

[26] **Skow, A.** (1992). Agility as a contributor to design balance, *Journal of Aircraft*, *29*(1), 34 – 46.

[27] **Le Blaye, P.** (2000). Agility: History, definitions and basic concepts, *Part of a report tile: Human Consequences of Agile Aircraft*.

[28] **van Oort, E.R.**, **Chu, Q.P.**, & **Mulder, J.A.** (2011). Maneuver envelope determination through reachability analysis, *Advances in Aerospace Guidance, Navigation and Control. Selected Papers of the 1st CEAS Specialist Conference on Guidance, Navigation and Control*. Berlin, Heidelberg: Springer Berlin Heidelberg.

[29] **Brandt, S.A.** (2004). Introduction to aeronautics: A design perspective (2nd ed.). Reston, VA: American Institute of Aeronautics and Astronautics.

[30] **Nguyen, L.T.**, **Ogburn, M.E.**, **Gilbert, W.P.**, **Kibler, K.S.**, **Brown P.W.**, & **Deal, P.** (1979). Simulator study of stall/post-stall characteristics of a fighter airplane with relaxed longitudinal static stability, *NASA Technical Paper 1538*, NASA.

[31] **Stevens, B.L.** & **Lewis, F.L.** (2003). Aircraft control and simulation (2nd ed.). Hoboken, NJ: John Wiley.

[32] **Baspinar, B.** & **Koyuncu, E** (2018). Aerial combat simulation environment for one-on-one engagement, *AIAA Modeling and Simulation Technologies Conference*, Kissimmee, Florida.

[33] **Allen, P.D.** (1993). Air combat model engagement and attrition processes high level design, *RAND Note N-3566-AF/A*, RAND.

[34] **Courter, R.W.** (2008). How the mustang trampled the luftwaffe: the role of the P-51 in the defeat of the german air force in world war two, *Ph.D. thesis*, Louisiana State University.

[35] **Kutschera, A.** (2000). Performance assessment of fighter aircraft incorporating advanced technologies, *Ph.D. thesis*, Loughborough University, https://dspace.lboro.ac.uk/2134/7545.

[36] **Paranjape, A.A.** & **Ananthkrishnan, N.** (2005). Combat aircraft agility metrics - a review, *Journal of Aerospace Sciences* & *Technologies*, *58*(2).

[37] **Kutschera, A.** & **Render, P.M.** (August 1999). Performance assessment of thrust vector controlled post stall maneuverable fighter aircraft using minimal input data, *AIAA-99-4020, AIAA Atmospheric Flight Mechanics Conference*.

[38] **Burgin, G.H.** & **Sidor, L.B.** (1988). Rule-based air combat simulation, *NASA Contractor Report 4160*, Titan Systems, Inc.

[39] **Nolin, P.C.** (2013). The future of combat aircraft: towards a 6^{th} generation?, *Draft Special Report of Science and Technology Committee*, NATO Parliamentary Assembly.

[40] **Anon.** (1979). Fighter combat comparisons No. 1, Grumman F6F-5 Hellcat vs. Mitsubishi J2M3 Model 21 Raiden ('Jack'), *Tacitus Publications*, New Jersey, USA.

CURRICULUM VITAE

Name Surname: Nazmia Humaira

Place and Date of Birth: Jakarta, 8 July 1993

E-Mail: humaira@itu.edu.tr

EDUCATION:

- **B.Sc.:** 2016, Istanbul Technical University, Electrical & Electronics Engineering Faculty, Control & Automation Engineering
- **B.Sc.:** 2015, Istanbul Technical University, Aeronautics & Astronautics Faculty, Aeronautical Engineering
- 2016, Universidad Politecnica de Madrid, ATM Safety Challenges
- 2014, ENSTA ParisTech, Vehicle Dynamics
- 2014, Institut Polytechnique des Science Avancees, Aeronautical Engineering
- 2013, ETH Zurich & Paul Scherrer Institute, Energy Perspectives: Present & Future Technologies
- 2010, Universitas Indonesia, Metallurgy & Materials Engineering

PROFESSIONAL EXPERIENCE:

- 2014 Airworthiness Engineer at Regio Lease, France.

PUBLICATIONS:

- Saltoglu, R., Humaira, N., Inalhan, G., 2016. Maintenance Stop Time Influence on Aircraft Total Maintenance Cost with Downtime Integrated Cost Model. *7th International Conference on Mechanical and Aerospace Engineering (ICMAE)*, 2016, London, UK.
- Saltoglu, R., Humaira, N., Inalhan, G., 2016. Aircraft Scheduled Airframe Maintenance and Downtime Integrated Cost Model, *Advances in Operations Research,* doi: 10.1155/2016/2576825.